von KARMAN INSTITUTE
FOR FLUID DYNAMICS

TECHNICAL NOTE 53

ON SOME PROPERTIES OF REATTACHING LAMINAR AND TRANSITIONAL HIGH SPEED FLOWS

by

Jean J. GINOUX, Professor
von Karman Institute,
and
Brussels University

RHODE-SAINT-GENESE, BELGIUM

SEPTEMBER 1969

von KARMAN INSTITUTE FOR FLUID DYNAMICS

TECHNICAL NOTE 53

ON SOME PROPERTIES OF REATTACHING LAMINAR AND TRANSITIONAL HIGH SPEED FLOWS

by

Jean J. GINOUX, Professor
von Karman Institute,
and
Brussels University

A review paper presented at the 1969 international seminar on HEAT AND MASS TRANSFER IN FLOWS WITH SEPARATED REGIONS, in Herceg-Novi (Yougoslavia)

SEPTEMBER 1969

ABSTRACT

This paper is a review of some of the work done at the von Karman Institute over the past years on separated flows. Emphasis is given on a fundamental phenomenon developing in reattaching high speed flows, namely, spatially periodic patterns of counter-rotating streamwise vortices. Detailed surveys made with pitot-static tubes, hot wire probes, recovery temperature and heat transfer gages are presented. The effect of streamwise vortices on transition was studied using axisymmetric models on which the strength of vortices could be artificially controlled. For this purpose, a new criterion for transition detection was used. The effect of air and foreign gas injection in separated flow was studied and its application to suppressing local heat transfer peaks examined.

TABLE OF CONTENTS

LIST OF FIGURES

1. INTRODUCTION

There are many practical instances in which boundary layer separation occurs. This is particularly so in high speed flights because of the presence of shock waves. Shock wave boundary layer interactions exist for example at the compressor inlet of turbojets or ramjets, on deflected control surfaces, etc. on high speed vehicles.

After separation, mixing of the shear layer with the high speed external flow is often sufficiently large for the flow to reattach to the body surface, giving rise to a low velocity separation bubble imbedded in a supersonic stream. The effect of separation is generally detrimental inasmuch as it decreases the performance of devices where it occurs. However, it can be beneficial if used as a means of reducing aerodynamic heating of the surface of high speed vehicles.

Following Chapman's classification, three types of shock wave boundary layer interactions are considered, depending upon the location of transition. In fully laminar or turbulent interactions, the transition region is located either well behind reattachment or well upstream of separation. In transitional types of flow transition is located between separation and reattachment. In most practical aeronautical applications at subsonic and low supersonic speeds turbulent type interactions do exist. However, at high supersonic or hypersonic speeds and high altitudes transitional and laminar interactions are also of practical interest.

A considerable amount of work has been done both theoretically and experimentally in this field. It has been reviewed in excellent papers ([1], for instance). The present paper is limited to a review of some of the work done by the author on this problem during the past few years. Emphasis is laid on the discovery of spatially periodic patterns of streamwise vortices in reattaching boundary layers which produce important spanwise variations of boundary layer properties, in particular of heat transfer. The phenomenon is basically related to boundary layer stability and has application to high speed flights. In particular, a new phenomenon called "cross-hatching" has been systematically observed by other investigators on high speed ablating bodies, the origin of which is hypothesized to be the presence in the boundary layer of an array of regularly spaced counter rotating longitudinal vortices (2,3,4).

The present study is quite general as it covers a Mach number range of 1.5 to 7.0 and flow separation caused by various types of steps and ramps on planar and axisymmetric bodies. The research was conducted at the von Karman Institute for Fluid Dynamics (Rhode Saint Genèse, Belgium) and sponsored in part by the Air Force Office of Scientific Research, through the European Office of Aerospace Research, OAR, United States Air Force, under Grants covering the period 1961-69, ending with the AF-EOOAR 69-0056.

2. EXPERIMENTAL EQUIPMENT

2.1 Wind tunnels

Five different supersonic and hypersonic wind tunnels (four being located at VKI and one at AEDC) were used to cover the Mach number range 1.5 to 7.0, as indicated in table I, where stagnation conditions and free stream Reynolds numbers are also shown.

Wind tunnel	M	Stagn.pres. psi	Stagn.temp. °K	Re per inch
S-1 (VKI)	2.21	2 to 4	288	$5.0\ 10^4$
S-2 (VKI)	1.5	14	288	$3.7\ 10^5$
	2.15	14	288	$3.3\ 10^5$
S-3 (VKI)	2.67	56	288	$9.5\ 10^5$
H-1 (VKI)	5.3	450	373	$1.4\ 10^6$
	6.0	450	450	$8.0\ 10^5$
	7.0	450	623	$3.2\ 10^5$
D (AEDC)	3.0	2 to 30	295	0.03 to $0.4\ 10^6$

Table I

S-1 is a continuous closed circuit wind tunnel which has a test section of 40 × 40 cm² (16"×16"). It is operated at stagnation pressures lower than atmospheric. The stagnation temperature has approximately the room value.

S-2 is a very small continuous wind tunnel with a test section of 15 mm × 15 mm (i.e., about $\frac{1}{2}$ " × $\frac{1}{2}$ "). Dry air is sucked in through the nozzle by the vacuum pump that is used to maintain tunnel S-1 at its low pressure level. In this tunnel, tests were made on backward facing steps machined directly in the nozzle block itself.

S-3 is a blowdown tunnel ejecting air to the atmosphere. With the compressed air available it can practically be operated as a continuous facility. It has a test section of 5×6 cm^2 (i.e., 2" × 2.5").

H-1 is a blowdown tunnel with an effective test section of 120 mm × 120 mm (i.e., about 5" × 5"). It is equipped with a contoured rectangular nozzle for $M = 5.3$ and wedge tilt blocks for the Mach number range 6 to 8. The running time is of about 5 minutes at a stagnation pressure of 450 psi. The exhaust pressure can be lowered to 7 psi absolute by a supersonic ejector using the same air supply. A pebble bed preheats the air up to 500 °C maximum.

Tunnel D is a 12 × 12 in. supersonic blow down facility located at the Arnold Engineering Development Center in Tullahoma (Tennessee, U.S.A.). It was used at a Mach number of 3 although it can be operated in the range 1.5 to 5 with stagnation pressures from 2 to 30 psi. The running time is of the order of several minutes with exhaust into a vacuum tank.

2.2 Models

Models of various sizes and configurations were used in the different wind tunnels which are fully described in the references listed at the end of the present paper. Main dimensions will be indicated in the text when they appear necessary.

2.3 Test techniques

Each tunnel is equipped with its own schlieren and shadow system. Flow pictures were taken with spark light sources of small duration time.

Surface flow visualizations were made by a sublimation technique using azobenzene or acenaphtene as indicators. The response time varied between a few seconds and a couple of hours depending upon the type of indicator, its thickness and the flow conditions. The fluorescent oil technique was also used.

Static and pitot pressures were measured by differential pressure transducers. For static pressure distributions rotary valves and a single transducer were used.

Detailed surveys were made with small total-head and static probes. The pitot tubes were cylindrical with circular noses and the static probe was a cone cylinder having one single pressure orifice, located on its starboard side, twelve diameters behind the nose. The probes were fixed to surveying micromechanisms that permitted displacements parallel and perpendicular to the surface of the models at any streamwise location.

Spanwise variations of heat transfer in the reattachment region of the flow behind a forward facing step were measured with a transient calorimetric technique (6). Streamwise distributions of recovery temperature were measured on araldite (thermal insulator) models in which thermocouples were imbedded flush with the surface (7).

Hot wire surveys were made at AEDC with a commercially available Shapiro-Edwards Model 50B hot-wire equipment. The mean-square voltage of the hot-wire output, given by a vacuum thermocouple, was recorded on an x-y plotter versus the spanwise location of the wire. The hot wires were 0.0003 in. diam. by 0.05 in. long tungsten wires, operated with a constant current of 25 ma (overheat ratio of 0.2). They were welded on 0.035 in. diam. sewing needles.

3. ON THE EXISTENCE OF STREAMWISE VORTICES

3.1 Surface flow visualization

Evidence of an orderly three dimensional behaviour of high speed reattaching flows on two dimensional models at low Reynolds numbers is shown on several photographs in figures 1 to 11 in which the free stream direction is from left to right. On these pictures, streetlike surface flow patterns were visualized by a sublimation technique sensitive to skin friction variations over the model surface. Dark streaks correspond to large friction coefficients. As seen, over the surface of a given model, spacing of the striations is remarkably constant. This tends tc suggest that disturbances of a given wave length are amplified, while others are damped out, when high speed flows separate and then reattach to solid walls.

Figures 1 to 11 cover a Mach number range of 1.5 to 7.0 with Reynolds numbers based on distance from model leading edge to separation of 10^5 to 10^6. They involve various model configurations giving laminar or transitional types of flows. The scale of each picture can be deducted from the characteristic dimension quoted in each legend, such as model span.

Flows over backward facing steps are shown in figures 1 to 5 at Mach numbers of 1.5, 2.25, 2.67, 5.3 and 7.0. The flow over a flat plate with a 20 mm thick leading edge (simulating a forward facing step) is presented in fig. 6 at a free stream Mach number of 2.25. The photograph of figure 7 represents the surface flow in the case of a forward facing step located 120 mm behind the leading edge of a flat plate. The Mach number of the uniform flow parallel to the plate was 2.02. The unit Reynolds number was 2.1×10^6 /m for which transition to turbulent flow occurred upstream of reattachment. Figure 8 shows the surface flow over a 7.5 deg flap mounted 80 mm behind the leading edge of a flat plate at M = 2.25 and for a tunnel stagnation pressure of 180 mm of mercury. In all these cases, except in figure 7, the flow was laminar or transitional at reattachment.

In the course of this investigation it was feared that the present phenomenon could be generated by a cross flow in the separated region caused by model side effects (finite span). The presence of side effects is visible in figure 8 as a typical example. Indeed, similar striation patterns were observed in the case of an apparently unseparated flow over sweptback wings (60° sweep) at M = 2.25 where cross flow was obviously present (5). This is illustrated in figure 9 where one also notes a backward facing step in the constant span portion of the model. The existence of streamwise vortices induced by cross flow was explained by Owen and Randall (8). For this reason, axisymmetric configurations such as hollow cylinder with flares were tested at zero incidence. Typical results are shown in figures 10 and 11 at Mach numbers of 2.25 and 5.3 respectively. They show the existence of similar striation patterns than on the planar models although side effects were inexisting.

To gain quantitative information about the phenomenon reattaching flows were surveyed with small pitot, static pressure and hot wire probes. These probes, aligned with the upstream flow direction were moved along the model span while kept in the boundary layer at constant distances from the model surface.

3.2 Pitot surveys

Figure 12 is a typical example (8,9) of results obtained approximately 10 millimeters downstream of reattachment in the flow behind a 10 mm high backward facing step. The free stream Mach number was 2.25 and the tunnel stagnation pressure 170 mm of mercury absolute. In this figure, the variations of pitot pressure in percent of the values measured at $z = 0$ are plotted versus the spanwise coordinate z which has its origin on the centerline of the model; y is the distance of the probe axis above the model surface, δ the measured boundary layer thickness[†] and x the streamwise location of the probe downstream of the step. Figure 12 shows that spanwise variations existed with irregular amplitude but with a remarkably constant spacing between pressure peaks and valleys. For $\frac{y}{\delta} = 1$ (i.e., at the outer edge of the boundary layer) the pitot pressure was very nearly constant. For decreasing values of $\frac{y}{\delta}$, the amplitude of pressure variations increased, passed through a maximum at about mid-thickness (near the critical layer) and then decreased until the minimum value of y, determined by the probe external diameter was reached. Direct measurements with a sliding surface equipped with pressure taps indicated small periodic variations of the

---

[†] *Very slight spanwise variations of the boundary layer thickness were observed indicating that the outer edge of the viscous layer was wavy. δ, given in figure 12 is a spanwise average value.*

wall static pressure, less than 1 to 5 percent (6). Figure 12 shows that the pressure peaks have fixed spanwise coordinates throughout the boundary layer thickness. Comparison with sublimation pictures indicated a systematic correspondence between the locations of these peaks and the dark striations along which skin friction is higher.

Similar measurements were made on the same model at different values of x. For each x, the value of $\frac{y}{\delta}$, for which the amplitude of the pressure variations was maximum, was selected. It is indicated in the upper part of figure 13 which represents a cross section of the model (plane x,y) and the corresponding pressure variations are shown in the lower part of the figure which gives the percentage variation of pitot pressure (abscissa) versus z (ordinate). This figure shows that weak and irregularly spaced disturbances exist upstream of separation. They are amplified and become spatially periodic when the flow reattaches. The amplitude increases until the transition region is reached and then slowly decreases in the turbulent flow region. Over the available model length the pressure peaks remain at fixed spanwise locations.

The ratio of average spanwise distance between successive pressure peaks to boundary layer thickness measured upstream of separation was remarkably constant over the Mach number range 1.5 to 7.0 for the various flow configurations; it was of about 2.5.

3.3 Static pressure surveys

Typical results of spanwise surveys made in the boundary layer with a static pressure probe are given in figure 14, where the reading of the probe in millimeters of mercury is plotted against the spanwise coordinate (z). The measurements were made at different distances (y) from the model surface, but only the results for y = 4.5 and 5.5 mm are shown, as they indicate an interesting "phase shift" (i.e., peaks on one curve correspond to valleys on the other one and vice versa). This proves, the static probe being sensitive to small cross flows, that a layer of streamwise counter rotating vortices existed at $3.5 < y < 4.5$ mm, as sketched in the figure. In some of the measurements, a second layer of vortices was observed closer to the wall.

It therefore appears that the present disturbances are caused by streamwise vortices regularly distributed in the reattaching boundary layers.

3.4 Hot wire surveys

Hot wire surveys were made by the author at the Arnold Engineering Development Center (11) on the flow over a 10 deg ramp mounted on a flat plate. The free stream Mach number was 3.0 and the unit Reynolds number varied between 0.03×10^6 to 0.4×10^6 per inch. These surveys were made at three stations downstream of the leading edge of the ramp (x = 0.8, 1.5 and 2.6 inches). All surveys showed spanwise variations of the mean-square voltage output of the wire, in some cases the variations being as large as 40 percent of the average spanwise value. These, contrary to the pitot pressure variations, were of a different type whether the flow was laminar, transitional, or turbulent.

Figure 15b shows typical results obtained in a region of the flow just prior to transition. The mean-square voltage output of the hot wire ($\overline{e^2}$) is plotted at an arbitrary scale versus the spanwise coordinate (z) whose origin is at the centerline of the flap. Each curve corresponds to a survey made at a different height in the boundary layer. It is seen that the $\overline{e^2}$ level first increased ($0.03 \leq y \leq 0.045$ in.) and then decreased ($0.045 \leq y \leq 0.11$ in.) as the probe was moved away from the wall. This change occurred at about mid-height in the boundary layer whose thickness was determined approximately from schlieren pictures ($\delta = 0.12$ in. in this case). This was caused by the existence of a critical layer of intense fluctuation energy concentration in the boundary layer.

Now, it is quite remarkable that the sign of the spanwise variation of $\overline{e^2}$ was reversed as the probe passed across the critical layer. This is clearly seen by comparing the spanwise distributions of $\overline{e^2}$ for $y = 0.03$ and 0.07 in. in figure 15b. It is seen by comparing figs 15a and 15b that the pitot pressure and the hot-wire, mean-square voltage output peaks have identical spanwise locations. Above the critical layer, the peaks on the hot-wire and pitot probe traces are opposed, whereas below the critical layer they are in phase.

A cross plot of the results in figure 15b is given in figure 16, where the lines of constant, mean-square voltage output of the hot wire ($\overline{e^2}$ = constant) are plotted in the physical plane (y,z), y is the vertical distance above the flap surface, and z the spanwise coordinate. Although more numerous surveys should have been made, it is seen that local fluctuation energy concentrations exist along the span, near the critical layer, obviously related to the presence of streamwise vortices in the flow.

In the laminar region of the flow ($p_t = 2.5$ psia, $x = 1.5$ in.) the mean-square voltage output of the wire increased continuously with distance of the probe above the flap showing no critical layer. Generally, no sign reversal of the spanwise variation of $\overline{e^2}$ was observed and both pitot pressure and mean-square output peaks had the same spanwise location throughout the entire thickness of the boundary layer.

In the turbulent region of the boundary layer (p_t = 7 psia, x = 1.5 in.) the mean-square voltage output of the wire decreased continuously as the probe moved away from the surface. The pitot pressure peaks then correspond to valleys in the $\overline{e^2}$ distribution and vice versa.

3.5 Heat transfer surveys

Periodic variations of pitot pressure along the model span, together with a nearly constant wall static pressure, indicate that the slope of the velocity profile at the model surface varies periodically along the span which implies similar variations of the skin friction as demonstrated by the sublimation technique.

By Reynolds analogy spanwise variations of the heat transfer coefficient are therefore expected. Now, it is quite possible that, because of this, the aerodynamic heating of the model surface becomes locally larger than in the rest of the flow. This was qualitatively suggested by some of the sublimation pictures which show larger sublimation rates, i.e., skin friction, in the reattachment region where striations appeared than further downstream in the turbulent zone (see for instance figure 2).

It was therefore decided to make direct heat transfer measurements in the reattachment region of the flow behind a backward facing step 8 mm high (6). Typical results obtained at a free stream Mach number of 2.25 and a tunnel stagnation pressure of 100 mm of mercury absolute are shown in figure 17 where the heat transfer coefficient (h) is plotted versus the spanwise coordinate z. To ease the experimental study (see next section on leading edge effect), the amplitude of the flow perturbations was varied artificially by gluing thin strips of cellulose tape to the model surface in the vicinity of the leading edge. These are seen in figure 18b and their locations are indicated by the shaded areas along the z-axis of figure 17.

Figure 17 shows the existence of large peaks in the heat transfer rate. These peaks are approximately 50 percent higher than the heat transfer coefficients measured in the fully turbulent region of the flow further downstream and they have the same location as the pitot pressure peaks (6). These findings were remarkably confirmed by Miller et alii (12) who observed regular striation patterns scorched into the stainless steel surfaces of their flap models during hotshot wind tunnel tests at high Mach numbers.

4. LEADING EDGE EFFECT

Small free stream non uniformities and model imperfections which are unavoidable under practical test conditions can trigger small disturbances in the boundary layer of the type measured upstream of separation (see fig. 13). As the flow separates and reattaches, a stability mechanism acts which organises them into a regular pattern causing the spanwise variations of boundary layer properties demonstrated in the previous sections.

This mechanism is remarkably illustrated in figure 18 which shows that strong disturbances caused by pieces of cellulose tape wrapped around the model leading edge led, after a certain distance behind reattachment, to the same regular pattern than with a "clean" leading edge. These tests were made at a free stream Mach number of 2.25 with a backward facing step 8 mm high. It is also demonstrated by the sublimation picture of figure 20 where striation patterns induced by single roughness elements are visible.

The triggering action of the leading edge is demonstrated quantitatively in figure 19 where the variations of pitot pressure measured behind backward facing steps are plotted versus the spanwise coordinate z (10). The mean thickness of the model leading edge (ε_m) as well as the amplitude ($\Delta\varepsilon$) of spanwise variations in leading edge thickness are indicated. As seen, reducing the size of leading edge irregularities decreases the amplitude of the spanwise variations of pitot pressure without changing notably the average distance between pressure peaks, i.e., the wave length of the phenomenon.

Assuming no influence of free stream non uniformities, extrapolation of the results showed that leading edge irregularities should be smaller than 1 to $\frac{1}{2}$ micron to maintain a two dimensional flow within one percent. This is of course impossible to achieve on practical wind tunnel models or airplane wings and the phenomenon is likely to be systematically present.

The effect of leading edge was further demonstrated by testing axisymmetric bodies such as ogive-cylinder-flare models, on which the finite size leading edge is replaced by a point (the nose). Sublimation technique and pitot surveys revealed neither striation pattern nor spanwise pressure variation which proved at the same time that free stream non uniformities were too weak in the present studies to trigger disturbances in the boundary layer.

5. EFFECT OF VORTICES ON STREAMWISE FLOW PROPERTIES

Evidence was given of the existence of streamwise vortices in reattaching high speed flows. They were shown to induce spanwise variations of the boundary layer properties. The question then is : do they affect the streamwise properties of the reattaching flow ? For instance, it is known that the pressure rise at reattachment associated by the ability of a shear layer to reattach to the model surface, is dominated by the rate of mixing between the shear layer and the external flow. It is thus possible that the boundary layer streamwise vortices modify this mixing rate and therefore affect the wall static pressure distributions.

To answer this question a "vortex free" (axisymmetric ogive-cylinder-flare) model configuration was used on which streamwise vortices could be reintroduced "artificially". Static pressure distributions were then measured with and without vortices and the results compared.

The possibility of inducing streamwise vortices in the boundary layer at reattachment by discrete roughness elements located upstream of separation was first examined. Figure 20 shows the effect of small spheres, of various diameters and streamwise locations, glued on the surface of a flat plate (the diameter of spheres was always smaller than the local boundary layer thickness). As seen, they form striation patterns, i.e., streamwise vortices, which under certain circumstances (see third sphere from portside of the model) multiply remarkably during separation and reattachment of the flow, over a backward facing step in this case. It was thus concluded that discrete disturbances could produce regular patterns of streamwise vortices at reattachment by proper selection of their number and size.(It should be noted that the numerous circular spots visible in figure 20, downstream of the step, are either greassy spots or static pressure taps and not roughness elements).

Two different approaches were then used to "artificially" produce regular patterns of streamwise vortices in the reattachment region of flows over pointed nose axisymmetric bodies. In one case, (tests at a free stream Mach number of 2.25) the vortices were triggered by small jets of air of adjustable strength issuing normally to the model surface (13) and in the other case (tests at a free stream Mach number of 5.3), by small cylindrical roughness elements fixed to the model surface (14). The jets and roughness elements were distributed around the model in a cross plane located at the junction between the ogive and the cylinder, i.e., upstream of separation. The number (spacing) and size of these disturbances were systematically modified until nearly sinusoidal spanwise pitot pressure variations were measured downstream of reattachment, with an amplitude similar to those recorded on previous models with "natural" vortices.

This was achieved at M = 2.25 by 48 jets of air, 0.5 mm in diameter, spaced every 7.5 degrees (i.e., every 6 mm) around the model whose cylindrical portion had a diameter of 92 mm. The sublimation photograph of figure 21 shows the striation pattern obtained on the flare surface under these conditions. Figure 22 gives the corresponding peripheral distribution of pitot pressure measured in the boundary layer downstream of reattachment. p_p is the pitot pressure, z (or θ) the peripheral coordinate in millimeters (or degrees), p_t the tunnel stagnation pressure and p_{inj} the pressure difference in millimeters of mercury that controls the intensity of the jets. Measurements made upstream of separation but downstream of the jets plane revealed only very slight peripheral pitot pressure variations in the boundary layer. This demonstrated, as previously observed with "natural" disturbances, that the mechanism of separation and reattachment amplifies initial disturbances to produce strong fluctuations of a given wave length after reattachment. It is, however, unclear how the free shear layer amplifies the disturbances and more research is required to explain this.

At a free stream Mach number of 5.3, 32 cylindrical roughness elements were spaced every 11.2 degrees (i.e., every 3 mm) around the model whose cylindrical portion had a diameter of 30 millimeters. The optimum height of the roughness elements was 0.2 millimeters (which is smaller than the local boundary layer thickness) with a fixed diameter of 0.5 millimeters. The sublimation photograph of figure 23 shows the striation pattern obtained on the flare surface under these conditions. Figure 24 gives the corresponding peripheral distribution of pitot pressure.

Wall static pressure distributions were then measured in a meridian plane on each of the two models with and without vortices, using 0.2 mm roughness as well as shorter and taller ones. Differences of a few percent only (i.e., slightly larger than the usual experimental scatter were noticed at low Reynolds numbers, the tendency being to reduce the separation length with increasing roughness size. At higher Reynolds numbers slightly larger differences were noticed (see also next section).

It was thus concluded that streamwise vortices had little effect on the wall static pressure distribution when the free stream unit Reynolds number was sufficiently small.

Similar tests are presently being planned to verify the effect of streamwise vortices on the streamwise distribution of heat transfer, and in particular, to answer the question: "are the local peaks compensated by local troughs such that the heat transfer value averaged over the span is not much affected by the streamwise vortices ?"

6. EFFECT OF STREAMWISE VORTICES ON TRANSITION

The above discussions seem to indicate that the phenomenon observed in the present investigation is essentially one of instability in the two-dimensional flow. This three-dimensional configuration has been observed quite systematically in the process of transition from laminar to turbulent flow, at low speed by other investigators (15,16,17,18). It is thus of interest to further examine the effect of streamwise vortices on transition and, in particular, to determine if a shock wave boundary layer interaction reacts differently to changes in free stream Reynolds number with and without streamwise vortices in the reattaching shear layer.

To study such an effect one needs an accurate method of determining the type of interaction (laminar or transitional) than one is testing. Classical methods of detecting transition in unseparated flows (velocity profile, hot wire, recovery temperature, heat transfer measurements,etc.) are difficult to use or even inconclusive. This is firstly because flow properties (boundary layer velocity profile, etc.) are much distorted or affected by the strong pressure gradient that exists at reattachment and secondly, because even if the transition zone can be detected one still does not know by how much it can move upstream into the reattachment region for the type of interaction to change from purely laminar to transitional.

A demonstration of the drawback of such methods can be obtained from interesting results of recovery temperature measurements made at the von Karman Institute (7,19). It is a well known experimental fact that when a high speed laminar boundary layer over a flat plate becomes turbulent, the recovery temperature at the wall increases gradually from the laminar theoretical value (recovery factor equal to square root of Prandtl number) to the turbulent one (cubic root of Prandtl number) after passing through a slight peak near the end of the transition zone. A tentative to use this technique was made in flows over backward or upstream facing steps and flaps at a free stream Mach number of 2.25. This is illustrated in figure 25 and 26 for the case of backward facing steps (19). Step heights of 2.7, 5.1 and 6.8 millimeters and free stream unit Reynolds numbers of 1.4, 2.3 and 2.9 10^6 per meter were used. The recovery temperature (T_r) in degrees centigrade is plotted versus the distance x from the leading edge of the models. The steps were located at x = 120 mm. The theoretical values of T_r are indicated and appear generally lower than the measured values.

Figure 25a shows the results for a step of height of 2.7 mm for which the flow was laminar over the whole Reynolds number range. As seen, the recovery temperature decreases in the separated region behind the step and then increases back to its initial laminar flow value. For the 5.1 mm step, figure 25b demonstrates that the recovery temperature reached at the trailing edge of the model increases with unit Reynolds number until the turbulent value is reached. Then, by further increasing the Reynolds number, a peak develops which moves upstream. The peak further develops for the highest step height (fig. 25c) followed by a sharp decrease down to a value which is about equal to the initial laminar value, although from shadowgraph the flow appears to be turbulent.

Figure 26 shows the recovery temperature distribution when the boundary layer was made artificially turbulent upstream of separation. It again shows a peak in the reattachment region followed by a severe drop to low values. The subsequent rise of recovery temperature is then extremely slow.

This example, which reveals an unexpected flow property, illustrates the difficulty of using the recovery temperature distribution to determine the location of transition with respect to reattachment.

A direct method of detecting transition is the use of shadowgraphs. In laminar flows, the boundary layer appears as a white line which becomes fuzzy near the end of the transition zone. This method was refined by Chapman et al. (20) who noticed that in the transition region the white line was converging to the model surface (however, in the present tests this could never be clearly observed). Using this techniques, Chapman found that the static pressure measured at an arbitrary point <u>in the separated region</u> varied differently with Reynolds number in fully laminar and transitional cases. However, if there was indeed an obvious change in trend for the case of flows over steps, the situation was more confusing for flows over ramps. In these cases, the rate of change of the "plateau pressure" with Reynolds number was none but little affected (see for instance figure 20 of Chapman's report or figure 29 of the present study). These results were subsequently considered by some investigators as the basis of an indirect method of distinguishing between fully laminar and transitional separated flow.

There is a group of methods based on the presently well accepted fact (21,22,23) that the separation length increases (or decreases) when the flow is fully laminar (or transitional) while the abscissa x_0, at which the pressure starts to rise, decreases (or increases) when the free stream unit Reynolds number is increased. The separation length (ℓ_{sep}) is, as shown in figure 27, the distance between the separation (S) and reattachment (R) points on the dividing streamline (DSL).

However, S and R are extremely difficult to observe experimentally, and an accurate determination of x_0 would require a considerable number of pressure taps closely spaced.

A first attempt to develop a safer method was proposed by the author (11). It consisted in measuring, on shadowgraphs, the distance between the intersection points of the separation and reattachment shocks with the model surface as a function of free stream unit Reynolds number. In the present improved technique, the static pressure is measured at a given abscissa (x_N) near separation or near reattachment (where the pressure gradients are large and the pressure distribution nearly linear) as a function of tunnel stagnation pressure p_t (i.e., unit Reynolds number Re_u). This technique is different than Chapman's indirect method where the pressure is measured in the separated region.

The principle of this criterion is clarified by looking at figure 27, which shows schematically the observed trends of static pressure distributions as the free stream unit Reynolds number varies. These trends are suggested by results obtained in reference 23.

At low Re_u, the pressure distribution is shown by curve $A_1A_2A_3$. As Re_u increases, this curve moves into $B_1B_2B_3$ if the flow is laminar and then towards $C_1C_2C_3$ as transition moves upstream into the reattachment region. The corresponding variations of p_{x_N}/p_{e_0} are shown for x_N chosen near separation ($x_N \cong x_s$), in the separated region ($x_N \cong x_p$) and near reattachment ($x_N \cong x_R$) respectively. Cross plots (a) and (c) show a trend reversal while (b) does not. Selection of x_N near separation or reattachment is thus far superior to Chapman's choice made in the separated region.

A typical example of the results obtained by using this technique is shown in figure 28 where p_{x_N}/p_{e_0} measured in the separation region is plotted versus tunnel stagnation pressure in millimeters of mercury. The test was made at a free stream Mach number of 2.25 using a 10° flap mounted on a flat plate. The flap was located 60 mm behind the plate leading edge this distance being selected to cover both laminar and transitional types of flow. The theoretical variation of p_{x_N}/p_{e_0} based on Lees-Reeves-Klineberg theory (24,25) for fully laminar adiabatic flow is shown for comparison. As seen, the experimental data agrees with the theory at low stagnation pressures, but gradually departs from it as p_t increases. At $p_t = p_t^*$, the trend is reversed. It is concluded that above p_t^* the flow is certainly transitional and that the gradual departure between experiment and theory that occurs below this value might already be due to a gradual penetration of the transition zone into the reattachment region, including a possible effect of the streamwise vortices. The pressure measured in the separated region of the flow (as used by Chapman) is plotted versus p_t in figure 29. It is seen that it decreases over the whole range of p_t, even above p_t^* although at a slightly larger rate. By using the present method, the upper limit of free stream Reynolds number for the existence of fully laminar interactions at M = 2.25 was found to be 2 to 4 times smaller than quoted by Chapman et al.(20).

The present criterion was then used to study the effect of streamwise vortices on transition. Typical results are shown in figure 30 which gives the variation of p_{x_N}/p_{e_0} versus free stream unit Reynolds number at a free stream Mach number of 5.3. An axisymmetric ogive cylinder flare (vortex free) model was first used and the unit Reynolds number at which trend reversal occurred was noted (i.e., $Re_u = 3.3\ 10^5\ cm^{-1}$). Vortices were then introduced by 0.2 mm high roughness elements located as specified in the previous section and p_{x_N}/p_{e_0} was measured again versus Re_u. As seen in figure 30, the critical Reynolds number for trend reversal decreased to about 2.7 10^5/cm. This was confirmed by varying systematically the height of the roughness elements.

In conclusion, streamwise vortices that are present in the reattaching boundary layer decrease the value of the unit free stream Reynolds number above which the interaction becomes transitional, this decrease being more pronounced with larger roughness elements. In other words, streamwise vortices have a destabilizing effect.

7. EFFECT OF GAS INJECTION IN SEPARATED FLOWS

It was shown that streamwise vortices which are unavoidable in reattaching flows over planar bodies produce spanwise variations of boundary layer properties, in particular of heat transfer with large local peaks. For practical applications, it is of interest to develop a method of reducing these peaks, for instance, by injecting gas into the separated region of the flow. Therefore, experience was first gained at the von Karman Institute on the effect of gas injection in separated flows in the absence of streamwise vortices.

For a number of years it has been known that the presence of a cavity in the surface of a body gives rise to a significant redistribution of surface pressure and heat transfer to the body (26,27,28), Specifically, these quantities are reduced in the region of separated flow but experience a sharp increase (peak) within the vicinity of reattachment, followed by a decrease toward the undisturbed values in the downstream area. Nicoll (29) and the author (30) showed that it was possible to reduce or suppress these pressure and heat transfer peaks (thus retaining the interest of flow separation) by injecting small amounts of gas into the cavity. The author's study was made at a free stream Mach number of 5.3 on cone cavity models. Gas was injected into the cavity through an annular slot located near the cavity floor. Figures 31 and 32 show the distributions of pressure and heat transfer over the model surface in the region of reattachment without injection ($c_q = 0$) and with injection of air ($c_q \neq 0$). In these figures, c_q is the ratio of mass injection rate to boundary layer mass flow at separation, p and q are the local static pressure and heat transfer rate, p_c and q_c their cone values, x is the coordinate along the model surface as shown in the sketch and L is the cavity length. As seen, the pressure and heat transfer peaks decrease with increasing injection rate. Similar effects were obtained with foreign gas injection, light gases being more effective than heavy ones. The effect of the various gases on peak pressure ratio is summarized in figure 33, where K is a correlation parameter whose value is given in figure 34.

An attempt to use this gas injection technique in the case of reattaching flows with streamwise vortices was made at a Mach number of 2.25 by using a backward facing step model. Air was injected, normally to the surface upon which the flow was reattaching, through a 7 mm wide slot located near the step. The interior of the model, acting as a settling chamber for the injected air, was shaped in such a way that the velocity of injection was constant along the slot span within two percent. This was obtained in particular by limiting the slot span to one half the model span. Fences parallel to the upstream flow were introduced to isolate the central portion of the flow in which air was injected from the lateral portions.

The effect of injection was qualitatively observed with a sublimation technique. Remarkable results were obtained which are summarized in the photographs 35 to 37. Figure 35 shows the striation pattern caused by the streamwise vortices developing in the reattaching flow in the absence of injection. Note the fences and the injection slot which appears as a dark strip downstream of the step. Also note that the model leading edge does not appear on the photograph. Figure 36 shows that with a moderate amount of injection ($c_q = 0.4$, i.e., 40 percent of boundary layer mass flow at separation) a new striation pattern develops which try to match the one developing in the absence of injection. One should note that these sublimation results were obtained after running the tunnel for two to three hours and therefore that the phenomenon is very steady. Finally, at large c_q, figure 37 shows that the vortex pattern developing in the injected flow overruns the initial one.

Therefore, this technique does not look very promishing to reduce the effect of streamwise vortices on local heat transfer peaks.

8. CONCLUSIONS

An experimental investigation conducted in several wind tunnels at VKI and AEDC over a Mach number range of 1.5 to 7.0 revealed the existence of a basic phenomenon associated with boundary layer transition which develops systematically in laminar reattaching flows. Static pressure and hot wire surveys showed the existence of counter-rotating streamwise vortices located near the critical layer. These spatially periodic vortices are triggered by small and irregularly distributed leading edge imperfections and are producing important spanwise variations of boundary layer properties such as velocity profile, skin friction and heat transfer.

Vortex free configurations were developed in the form of axisymmetric bodies with pointed noses. Discrete roughness elements were used on these bodies to reintroduce "artificially" periodic streamwise vortices whose effects on wall static pressure distribution and transition were investigated. A new transition criterion was studied for that purpose, based on a change in trend of variation of some flow properties with free stream unit Reynolds number.

In transitional and turbulent reattaching flows, unexpected recovery temperature peaks were observed followed by unusually low values.

Gas injection into separated flow reduced pressure and heat transfer peaks existing at reattachment in some flow configurations, light gases being more efficient than air or heavier gases. The injected flow produced its own system of streamwise vortices which, at large injection rates, upset the vortex pattern that initially developed in the reattaching flow.

REFERENCES

1. CHARWAT, A.F.: Supersonic flows with imbedded separated regions. Advances in Heat Transfer, Vol. VI, Pergamon Press.

2. CANNING, T.N., WILKINS, M.E. & TAUBER, M.E.: Boundary layer phenomena observed on the ablated surfaces of cones recovered after flights at speeds up to 7 km/sec. AGARD CP No 19, vol. 2, May 1967.

3. CANNING, T.N., TAUBER, M.E., WILKINS, M.E. & CHAPMAN, G.T.: Orderly three dimensional processes in turbulent boundary layers on ablating bodies. AGARD CP No 30, May 1968.

4. TOBAK, M.: Hypothesis for the origin of cross-hatching. AIAA Paper No 69-11, January 1969.

5. GINOUX, J.: Instabilité de la couche limite sur ailes en flèche. Dédié au 60e anniversaire du Professeur Dr. H. Schlichting. Zeitschrift für Flugwissenschaften, 15 (1967),Heft 8/9.

6. GINOUX, J.: Streamwise vortices in laminar flows. AGARDograph 97 - Recent developments in boundary layer research. May 1965, Part I.

7. GINOUX, J.: Supersonic flow over flaps with uniform heat transfer. von Karman Institute, Belgium, VKI TN 30, Sept. 1966.

8. OWEN, P.R. & RANDALL, D.G.: Boundary layer transition on a swept back wing. RAE Addendum to TM Aero 277, 1952.

9. GINOUX, J.: Experimental evidence of three dimensional perturbations in the reattachment of a two dimensional laminar boundary layer at M = 2.05. von Karman Institute, Belgium, TN 1, November 1958.

10. GINOUX, J.: Leading edge effect on separated supersonic flows. Int. Council of Aeron.Sc. ICAS III, Stockholm 1964.

11. GINOUX, J.: Investigation of flow separation over ramps at $M_\infty = 3$. Arnold Engrg Development Center, Tennessee, AEDC TR 65-273, December 1965.

12. MILLER, D.S. et alii: Mach 8 to 22 studies of flow separation due to deflected control surfaces.
AIAA Jnl, vol. 2, No 2, February 1964.

13. LEBLANC, R.: Effets de rugosités sur écoulements laminaires décollés.
von Karman Institute, Belgium, Project Report 67-189, June 1967.

14. SCHNELL, W.C. & GINOUX, J.J.: Effect of surface roughness on axisymmetric laminar separated flows at M = 5.4
von Karman Institute, Belgium, TN 41, January 1968.

15. KLEBANOFF, P.S. & TIDSTROM, K.D.: Evolution of amplified waves leading to transition in a boundary layer with zero pressure gradient.
NASA TN D 195, 1959.

16. TANI, I.: Some aspects of boundary layer transition at subsonic speeds.
Adv. in Aer. Sc. (ICAS II), Vol. 3, 1962.

17. WALLIS, R.A.: Boundary layer transition at the leading edge of thin wings and its effect on general nose separation.
Adv. in Aer. Sc. (ICAS II), Vol. 3, 1962.

18. RUMSTADLER, P.W. et alii: An experimental investigation of the flow structure of the turbulent boundary layer.
Stanford Univ. Report MD-8, June 1963.

19. SANDFORD, J. & GINOUX, J.: Laminar, transitional and turbulent heat transfer behind a backward facing step in supersonic flow.
von Karman Institute, Belgium, TN 38, October 1968.

20. CHAPMAN, D.R., KUEHN, D.H. & LARSON, H.K.: Investigation of separated flows in supersonic and subsonic streams with emphasis on the effect of transition.
NACA TN 3869, March 1957.

21. LEWIS, J.E., KUBOTA, T. & LEES, L.: Experimental investigation of supersonic laminar, two dimensional boundary layer separation in a compression corner with and without cooling.
AIAA Jnl, January 1968, vol. 6, No 1, pp 7-14.

22. HOLDEN, M.S.: Theoretical and experimental studies of separated flows induced by shock wave/boundary layer interaction.
AGARD CP 4, Separated flows, May 1966.

23. GINOUX, J.: Supersonic separated flows over wedges and flares with emphasis on a method of detecting transition. von Karman Institute, TN 47, August 1968; see also Aerospace Research Labs, Ohio(USA), ARL 69-0009, January 1969.

24. LEES, L. & REEVES, B.L.: Supersonic separated and reattaching flows. I. General theory and application to adiabatic boundary layer/shock wave interactions. AIAA Jnl voL. 2, No 11, November 1964.

25. KLINEBERG, J.H.: Theory of laminar viscous inviscid interactions in supersonic flow. GLACIT, Ph.D. Thesis, 1968.

26. CHAPMAN, D.R.: A theoretical analysis of heat transfer in regions of separated flows. NACA TN 3792, 1956.

27. LARSON, H.K.: Heat transfer in separated flows. J.A.S. Vol. 26, pp 731-738, November 1959.

28. NICOLL, K.M.: A study of laminar hypersonic cavity flows. AIAA Jnl., vol. 2, No 3, pp 1535-1541, September 1964.

29. NICOLL, K.M.: Mass injection in a hypersonic cavity flow. Aerospace Research Labs (Ohio) - ARL 65-90, May 1965.

30. GINOUX, J.: Cone cavity flow at M = 5.3 with injection of light, medium and heavy gases. von Karman Institute,Belgium, TN 35, November 1968.

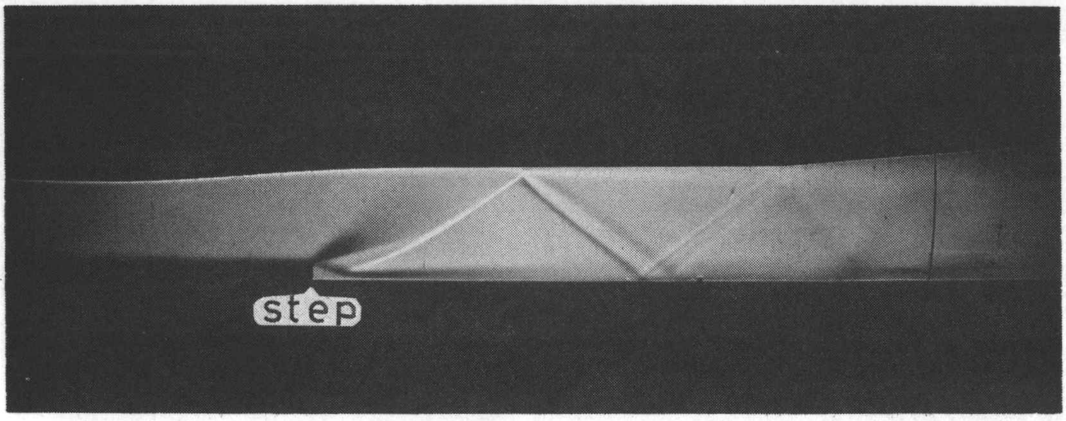

a) SCHLIEREN PHOTOGRAPH.

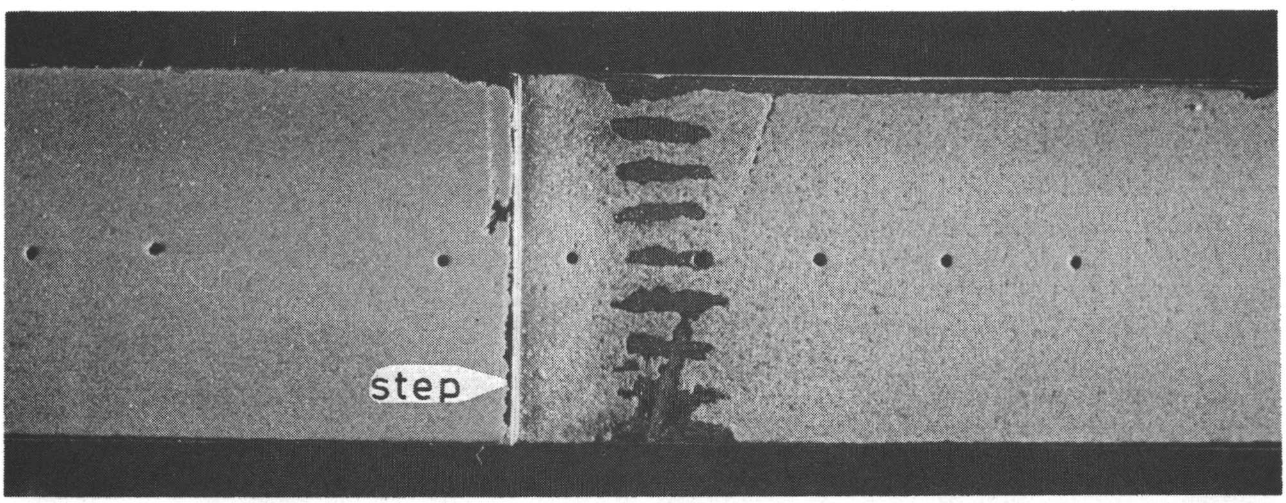

b) SUBLIMATION PICTURE.

FIGURE 1. FLOW OVER A 2mm BACKWARD FACING STEP AT M = 1.5 - MODEL SPAN : 15 mm.

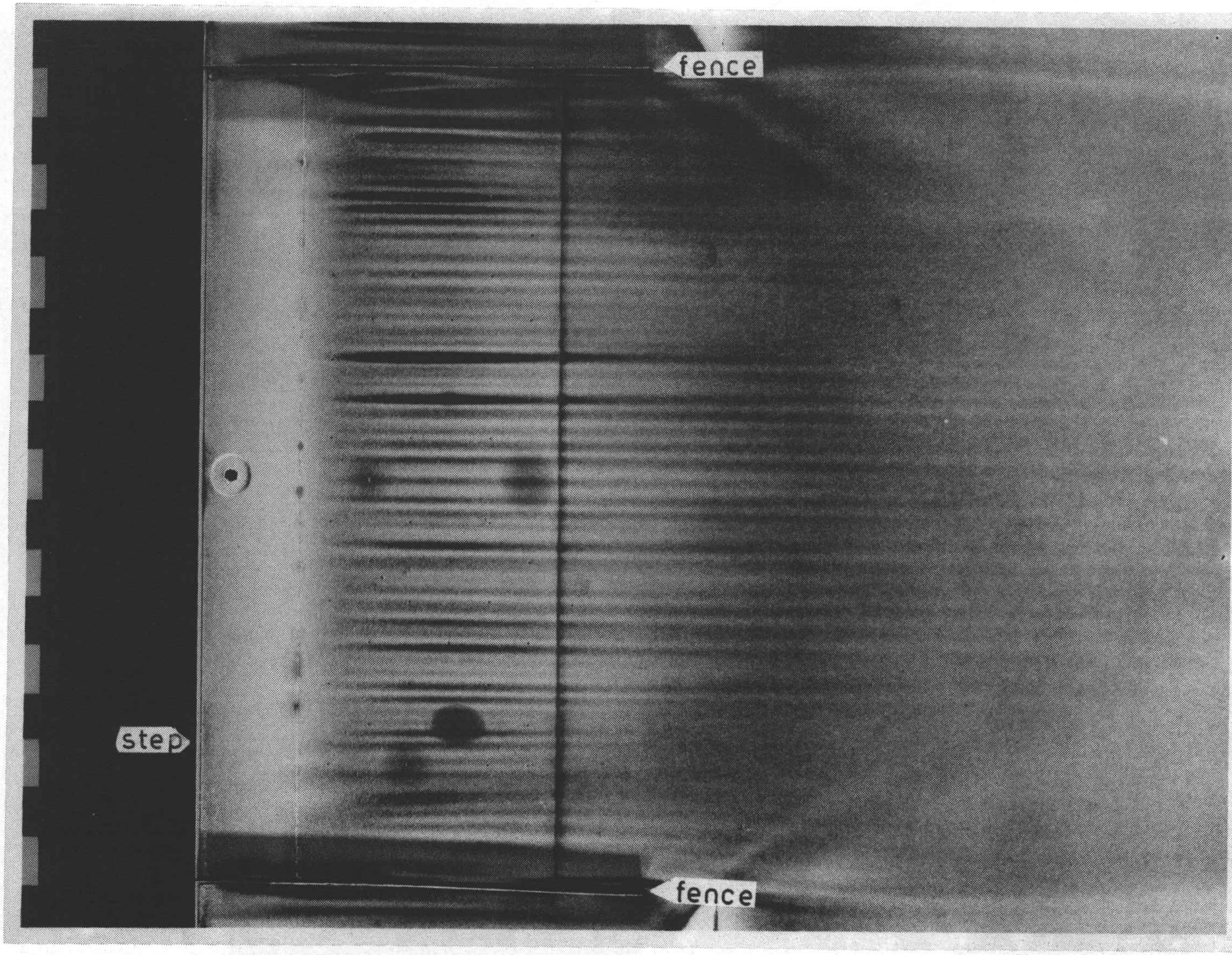

FIGURE 2. SUBLIMATION PICTURE OF THE FLOW OVER A 8mm BACKWARD FACING STEP AT M= 2.25 - DISTANCE BETWEEN FENCES : 150mm.

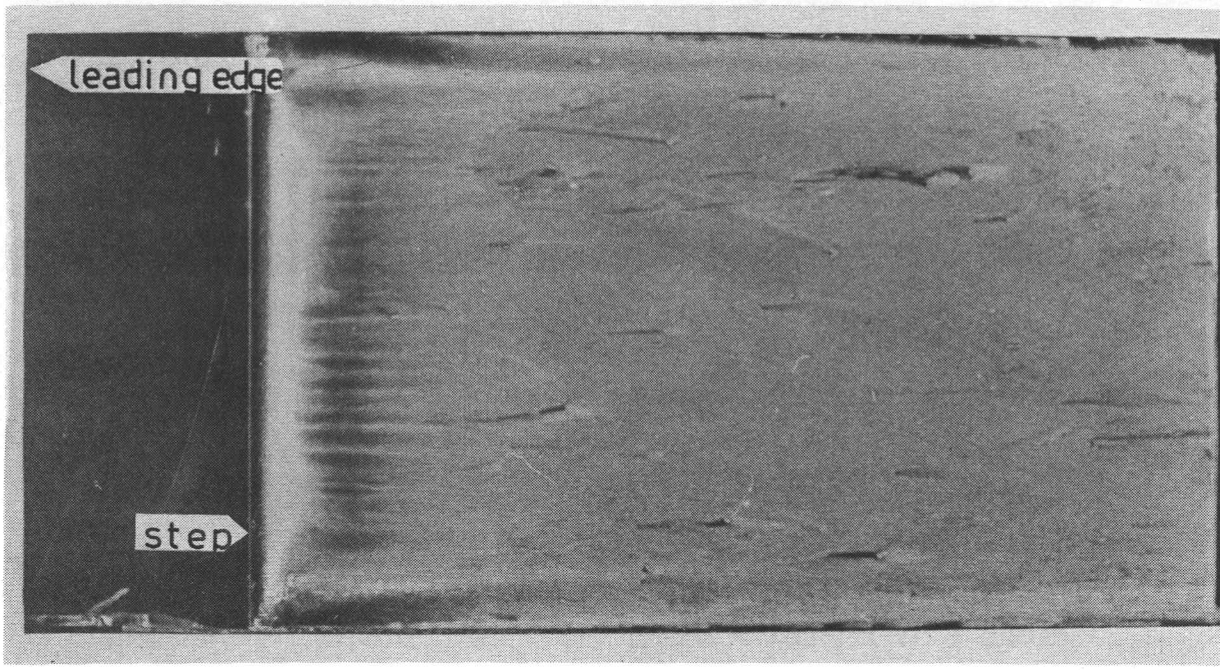

FIGURE 3. VISUALIZATION WITH FLUORESCENT OIL OF THE FLOW OVER A 2mm BACKWARD FACING STEP AT M=2.67 - MODEL SPAN: 50mm.

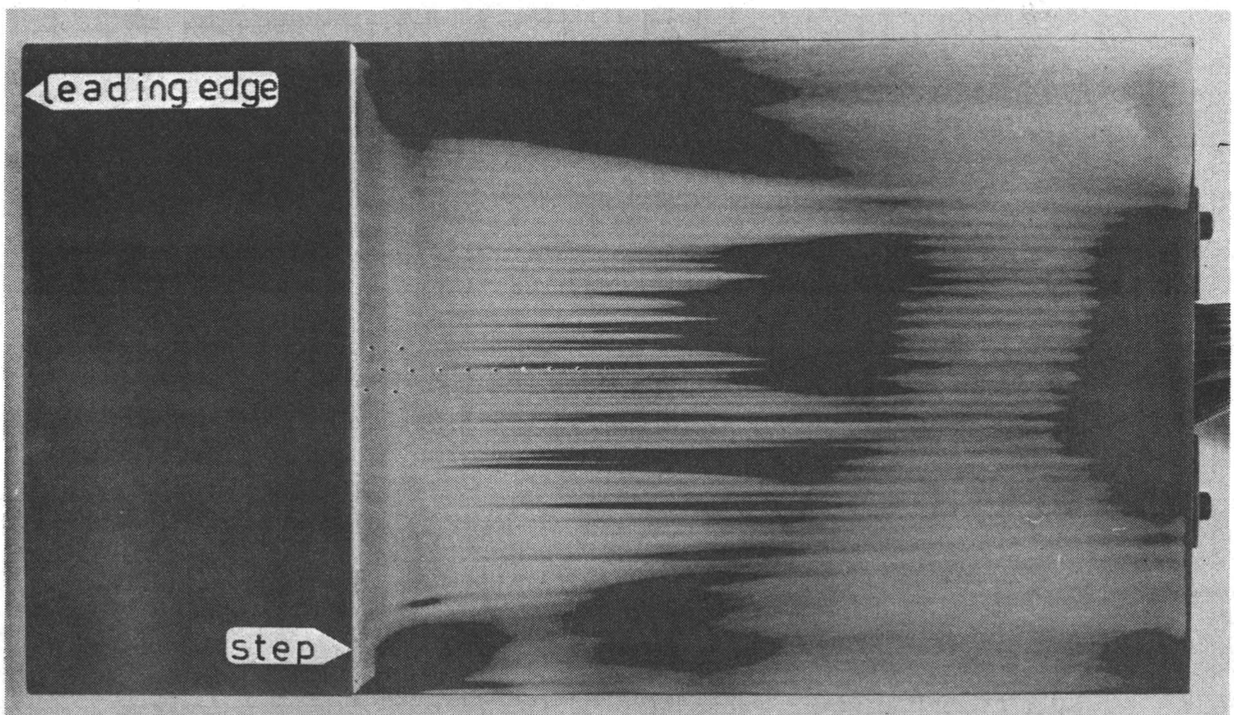

FIGURE 4. SUBLIMATION PICTURE OF THE FLOW AROUND A 2mm BACKWARD FACING STEP AT M=5.3 - SPAN : 120 mm.

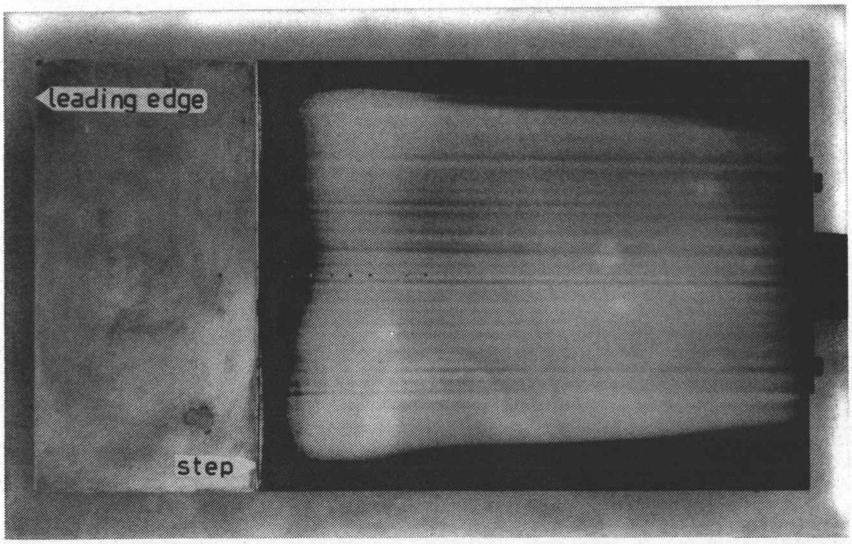

FIGURE 5. SUBLIMATION PICTURE OF THE FLOW AROUND A 2mm BACKWARD FACING STEP AT M= 7.0 SPAN :120 mm .

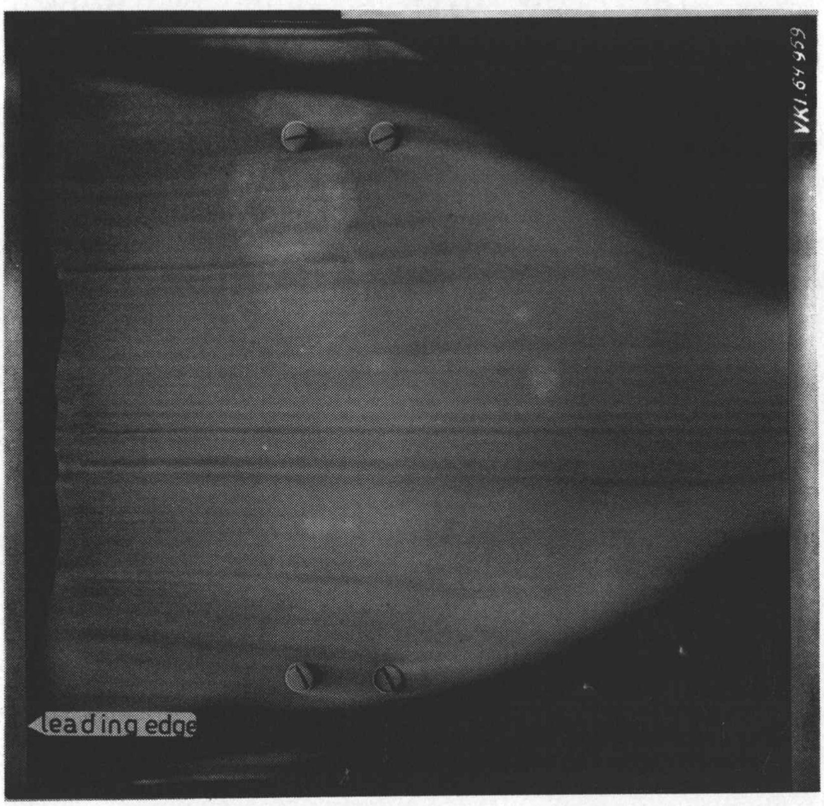

FIGURE 6. SUBLIMATION PICTURE OF THE FLOW OVER A FLAT PLATE WITH A LEADING EDGE THICKNESS OF 20mm. SPAN:300mm.

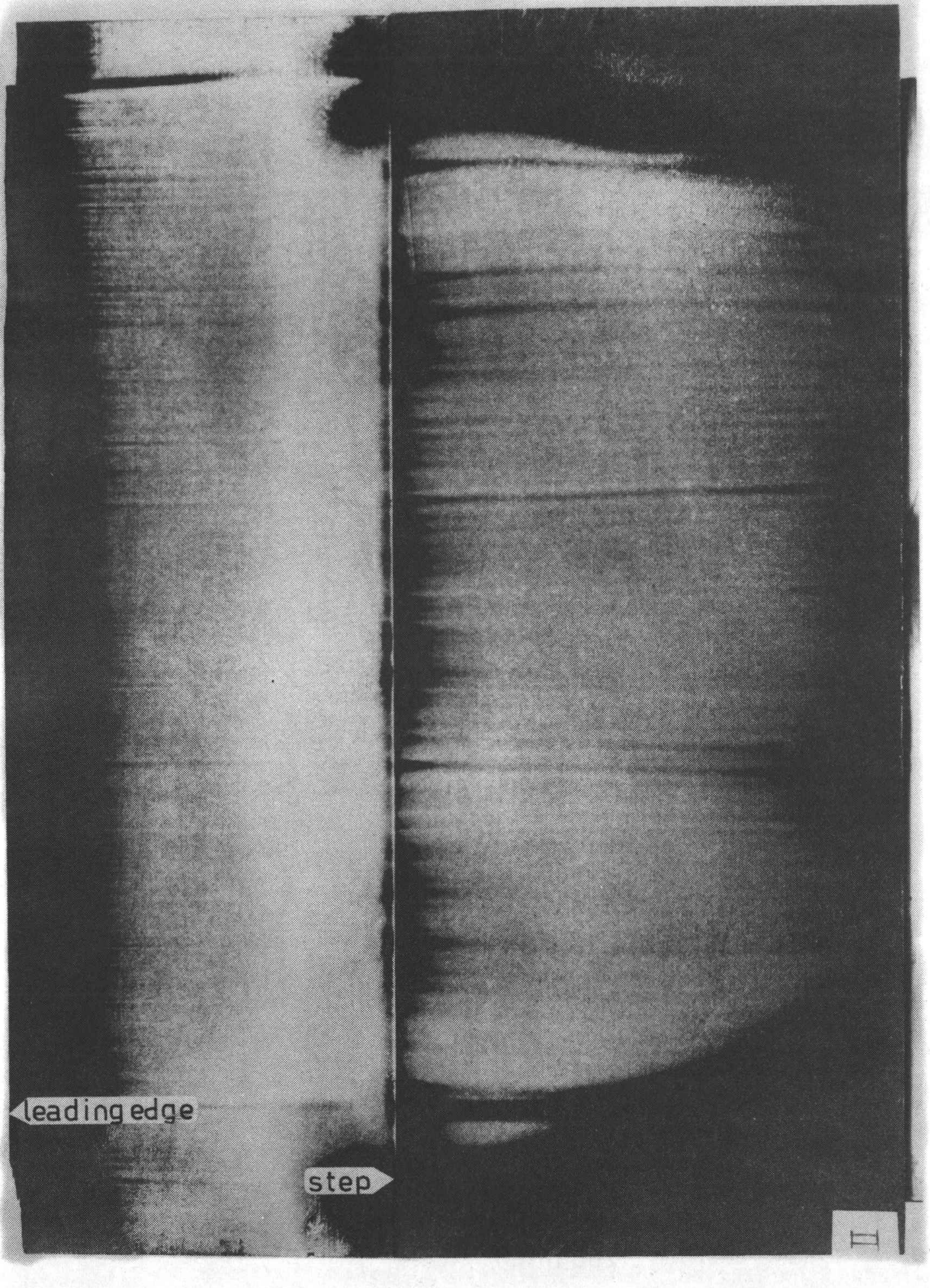

FIGURE 7. SUBLIMATION PICTURE OF THE FLOW AROUND A FORWARD FACING STEP AT M = 2.02
SPAN: 386 mm.

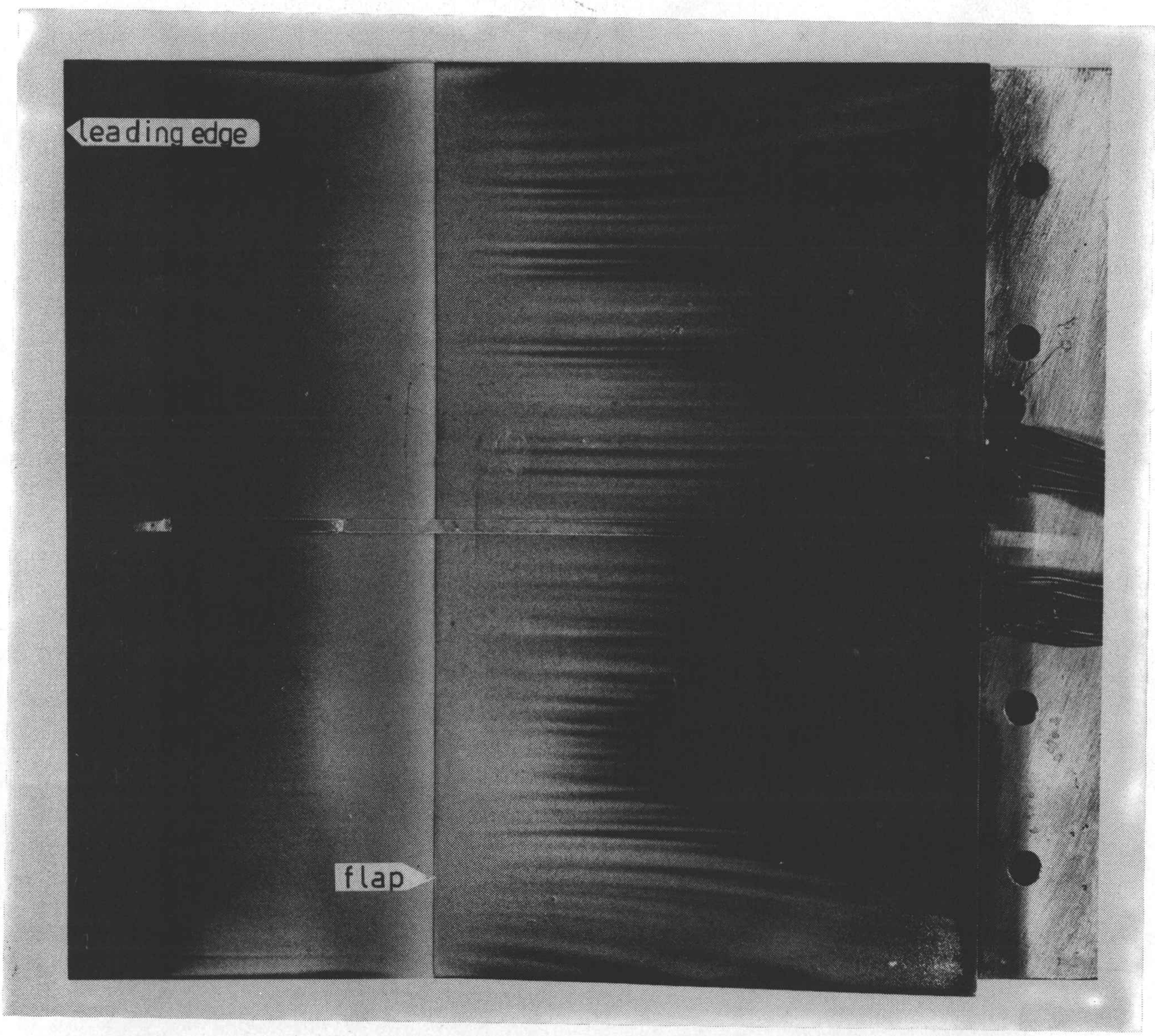

FIGURE 8. SUBLIMATION PICTURE OF THE FLOW AROUND A FLAT PLATE WITH FLAP AT $M = 2.25$
SPAN : 200 mm.

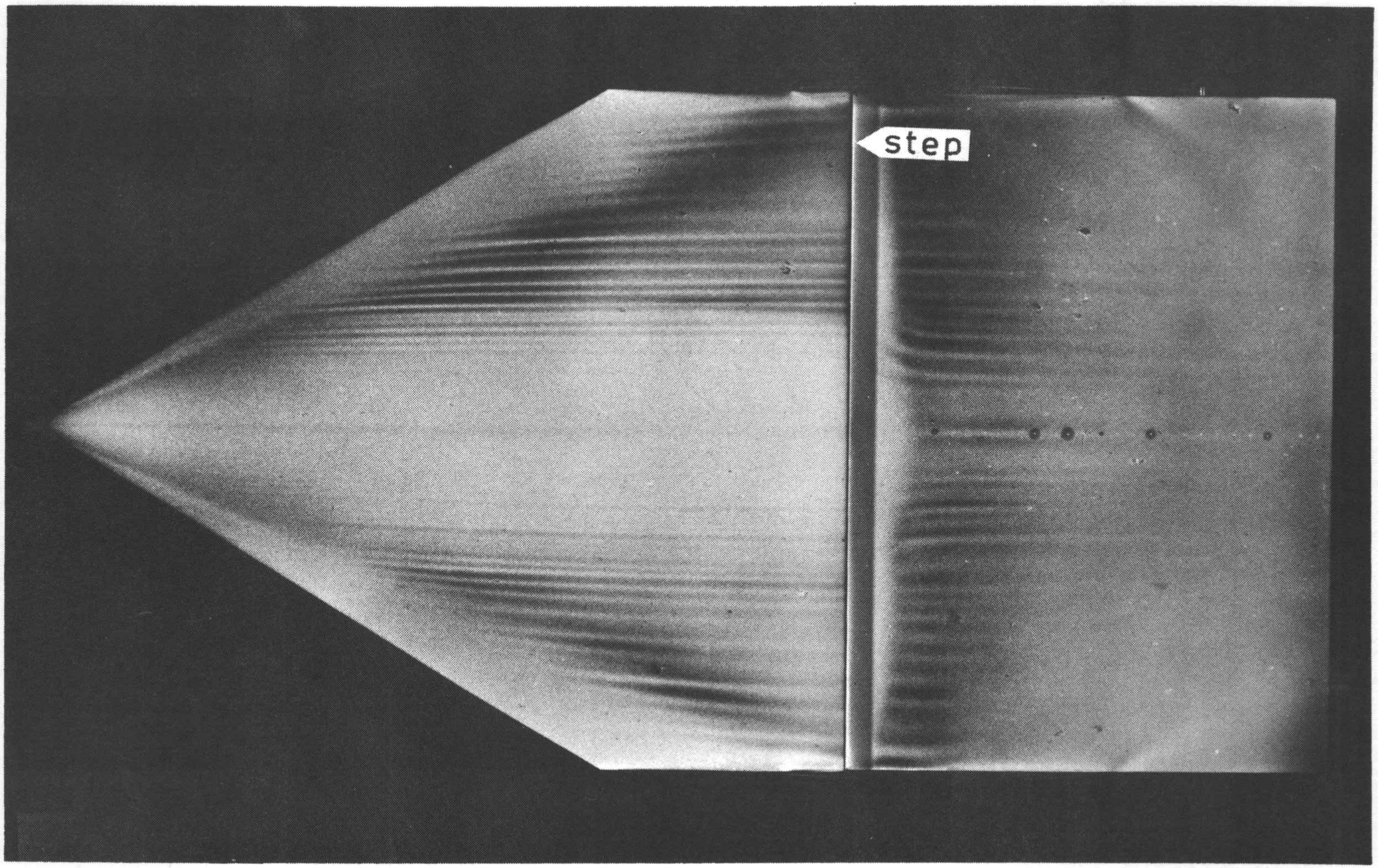

FIGURE 9. SUBLIMATION PICTURE OF THE FLOW AROUND A DELTA WING AND A 7mm BACKWARD FACING STEP AT M=2.25 - MODEL SPAN : 200 mm.

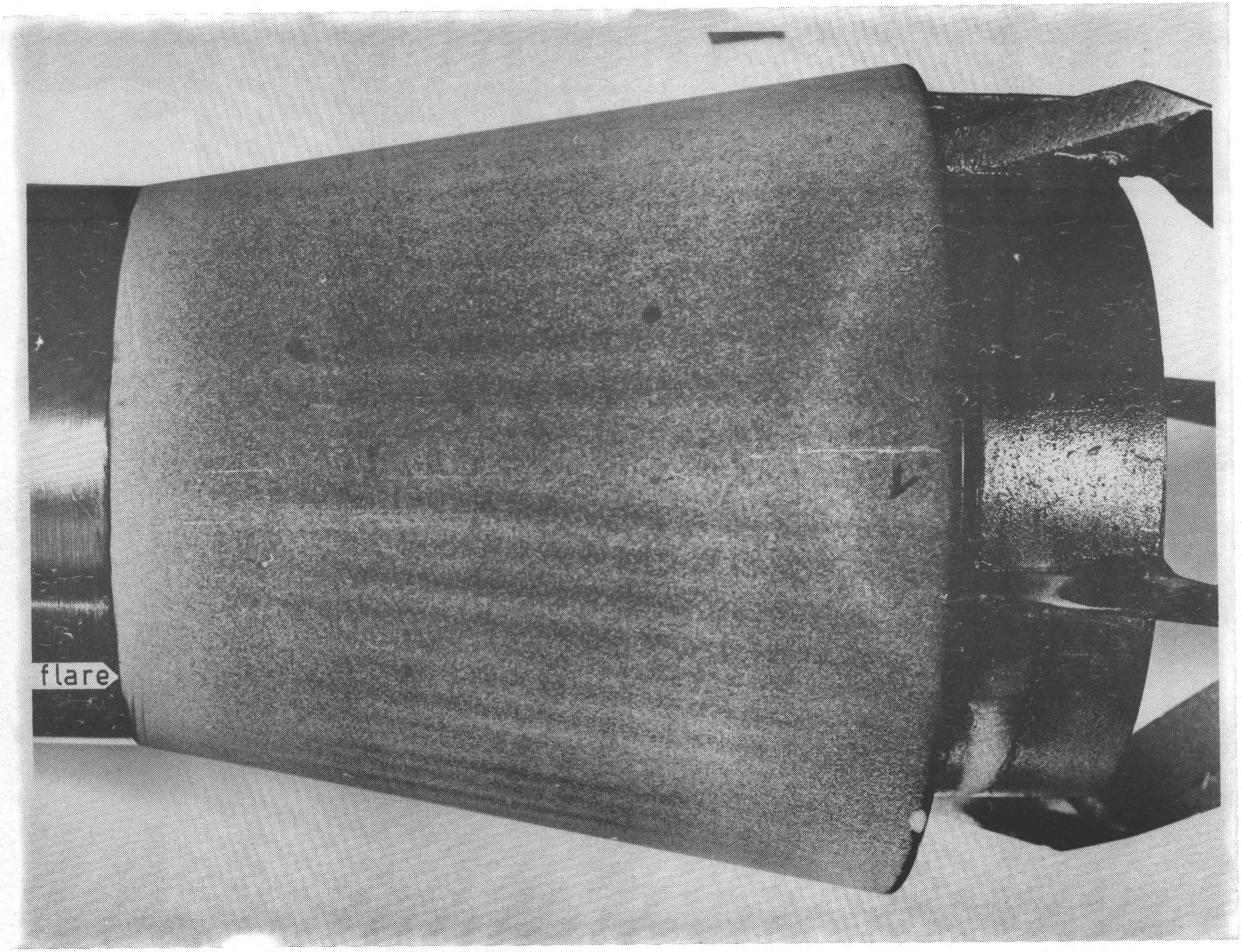

FIGURE 10. SUBLIMATION PICTURE OF THE FLOW OVER A 10° FLARE MOUNTED ON A HOLLOW CYLINDER AT M = 2.25 - CYLINDER DIAMETER: 100 mm.

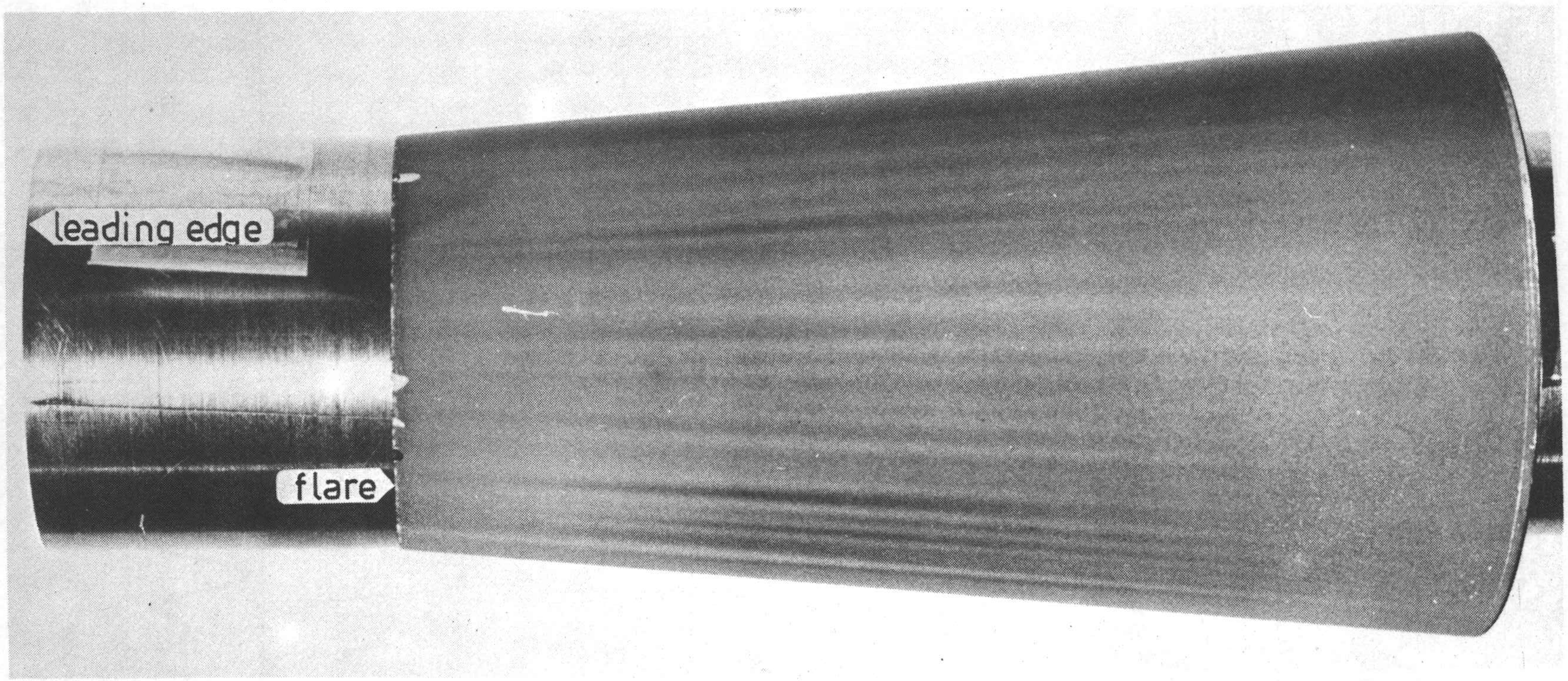

FIGURE 11. SUBLIMATION PICTURE OF THE FLOW OVER A 7.5 DEGREES FLARE MOUNTED ON A HOLLOW CYLINDER AT M = 5.3 - CYLINDER DIAMETER: 30 mm.

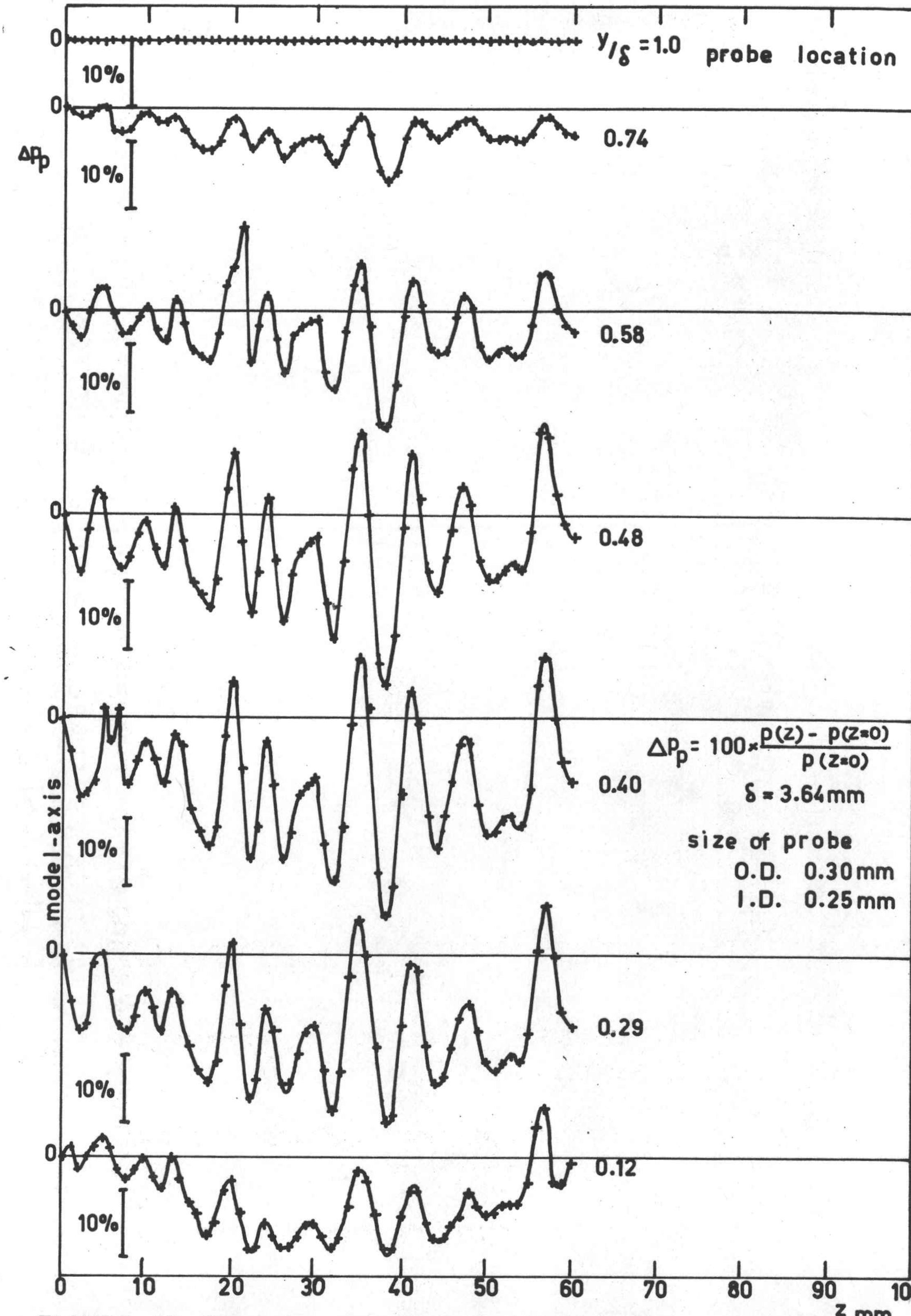

FIGURE 12 - Spanwise distributions of pitot pressure in the boundary layer behind a backward facing step

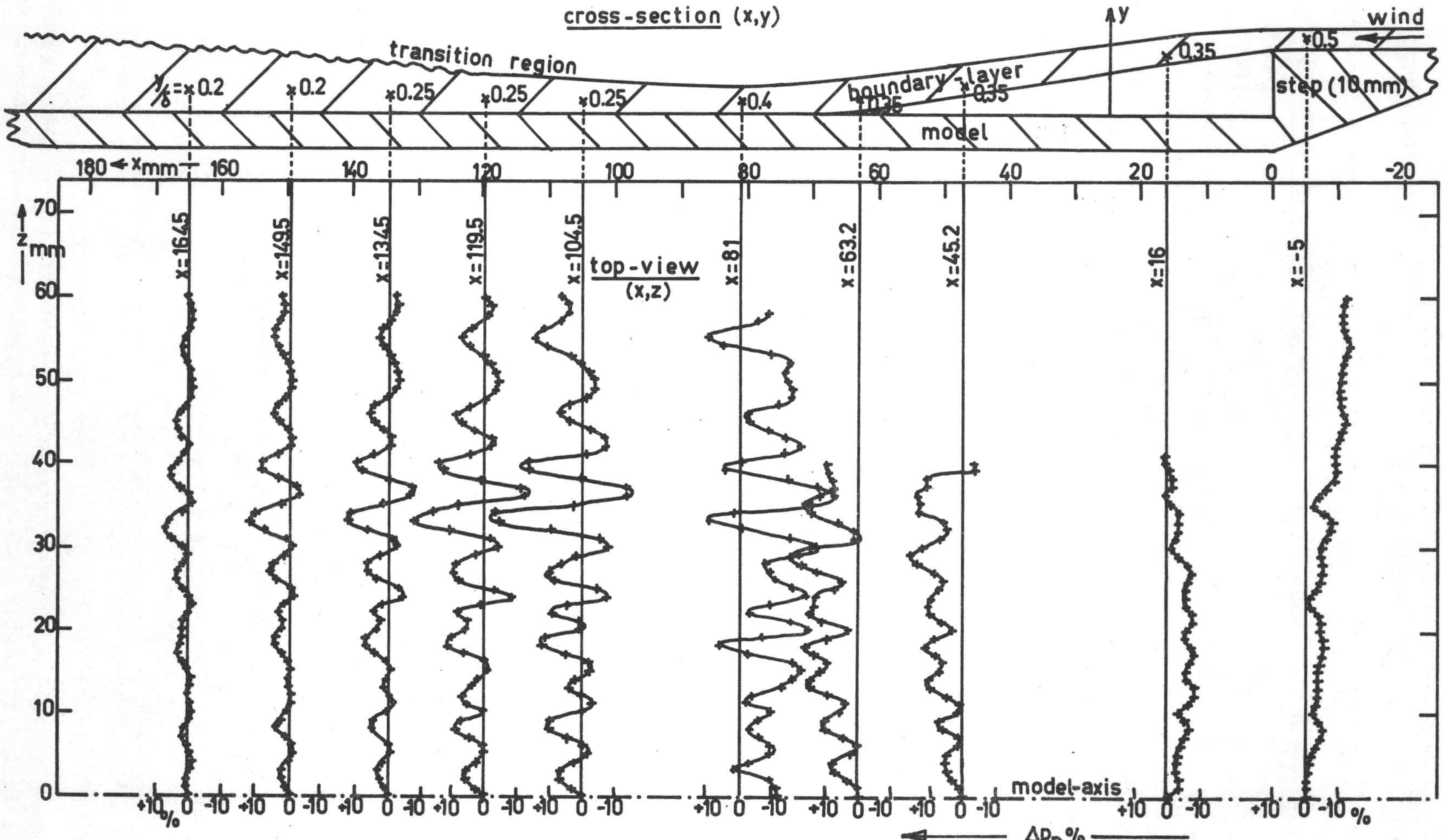

F I G U R E 13 – transverse variation of pitot-pressure at various x, in % of the pitot-pressure on model-axis.
measurements downstream of the step

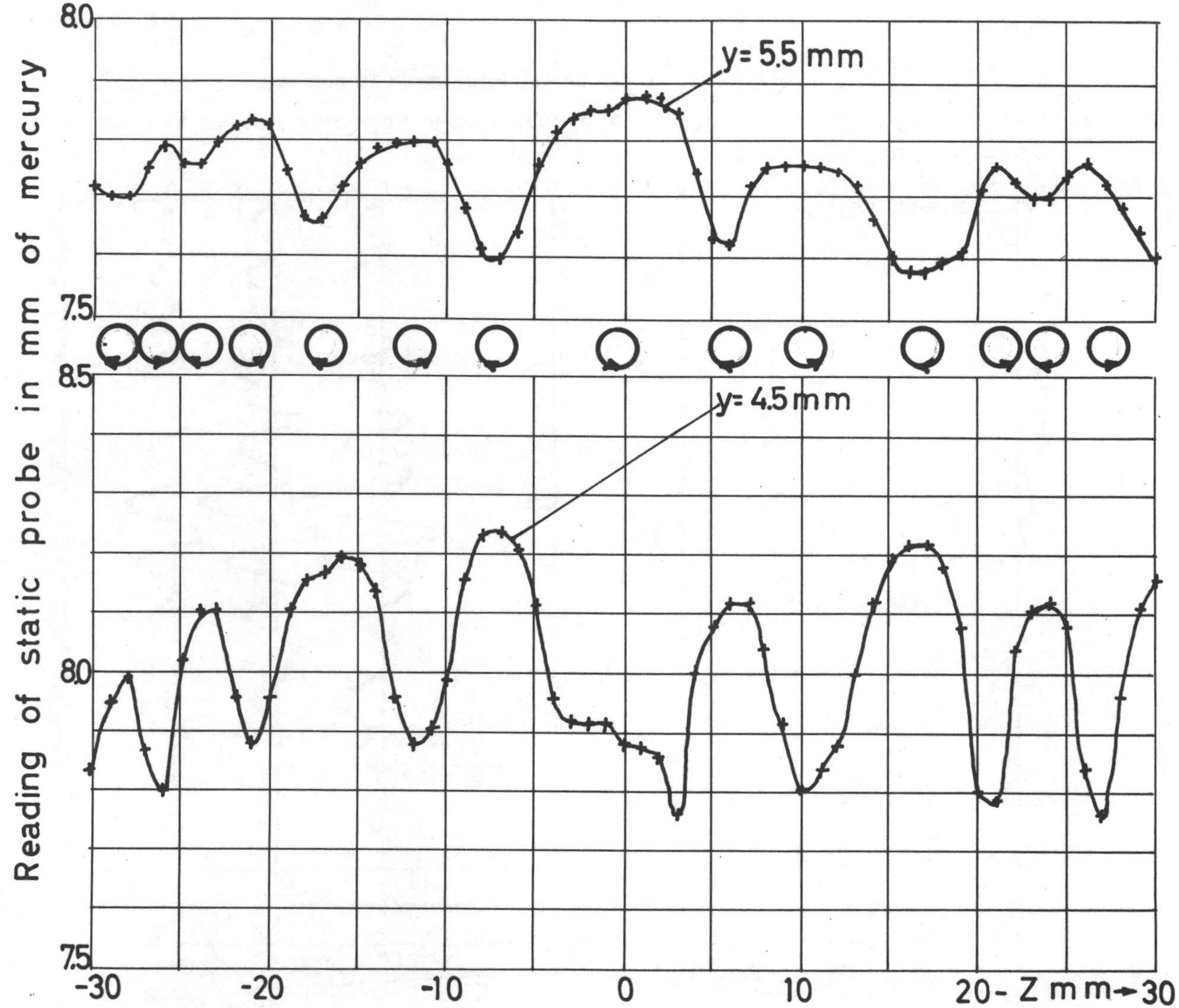

FIGURE 14 _ Spanwise surveys with static probe in the boundary layer behind a backward facing step

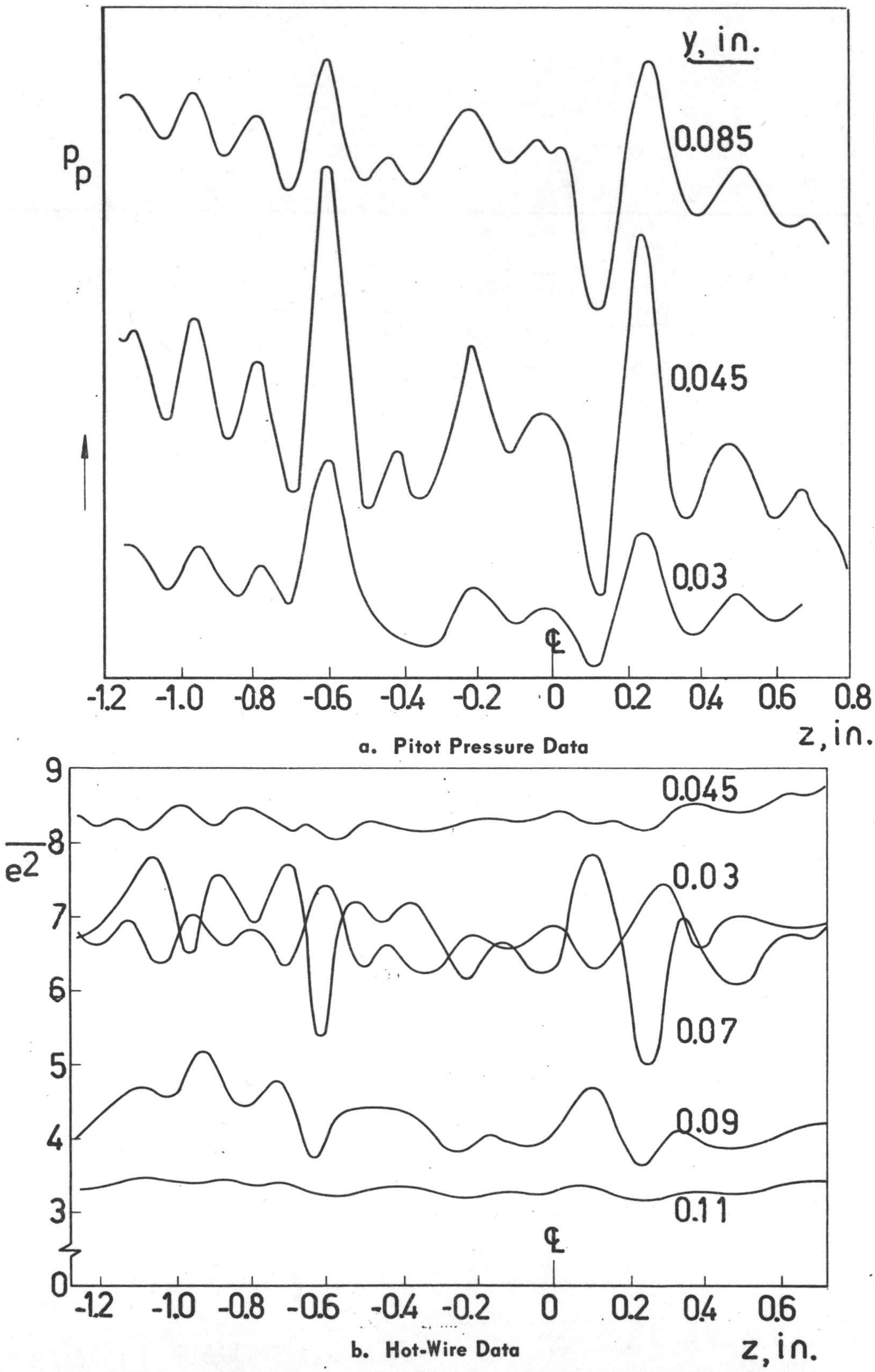

Fig. 15 Spanwise Variations of the Mean-Square Voltage of the Hot Wire and of the Pitot Pressure for a 10-deg Flap Angle; p_t = 4 psia, x = 1.5 in., and $\delta \doteq$ 0.12 in.

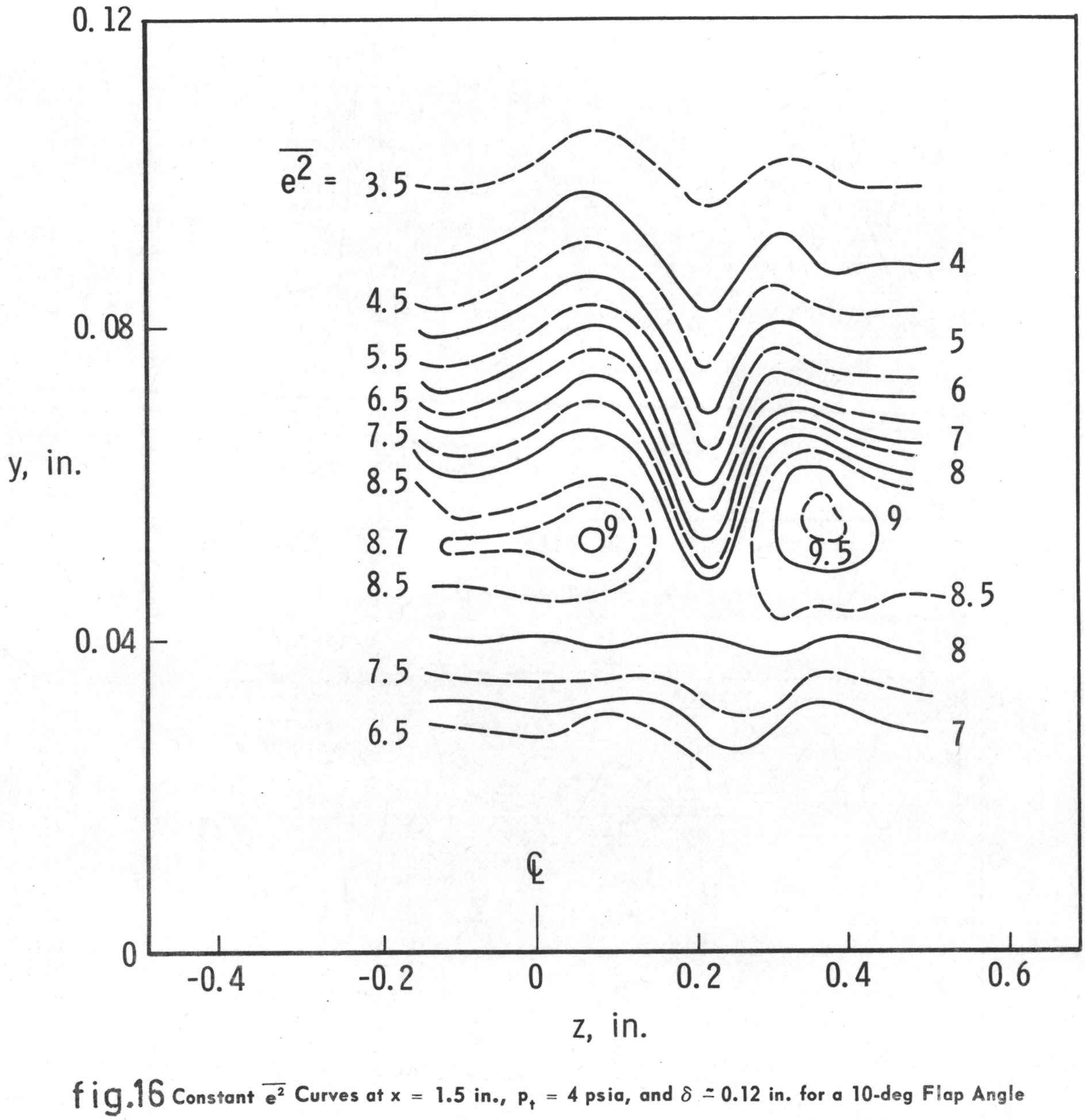

fig.16 **Constant $\overline{e^2}$ Curves at x = 1.5 in., p_t = 4 psia, and $\delta \doteq$ 0.12 in. for a 10-deg Flap Angle**

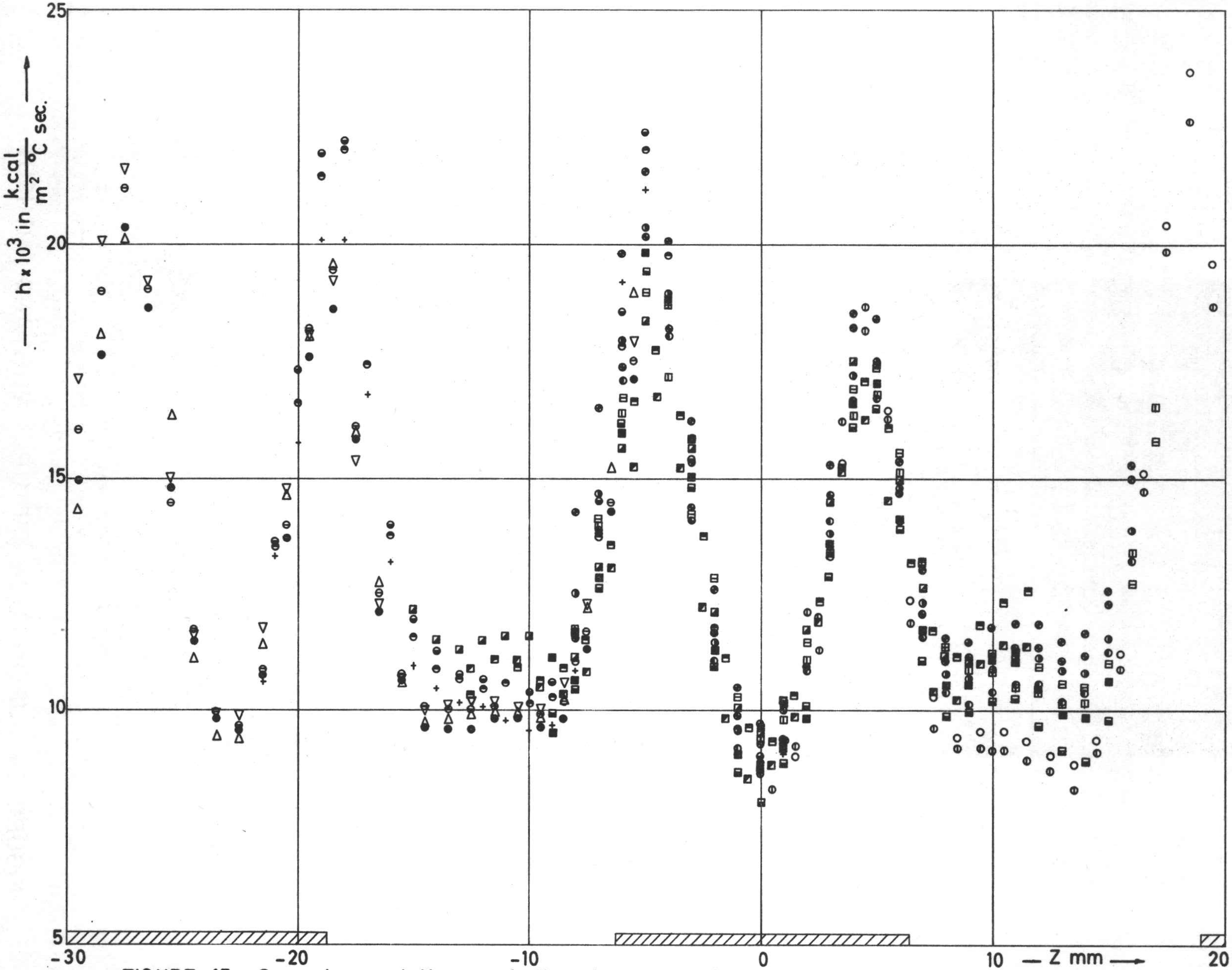

FIGURE 17 - Spanwise variations of the heat transfer coefficient - Summary of the results

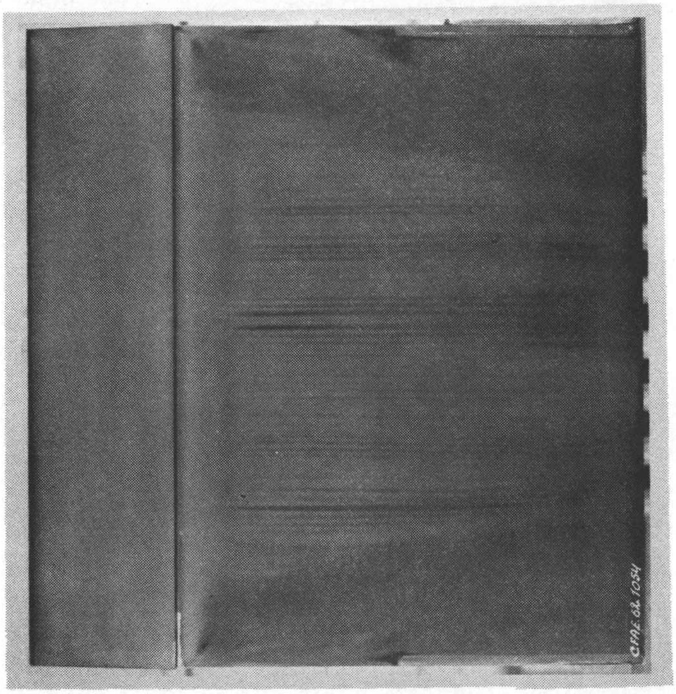

a) NO TAPES.

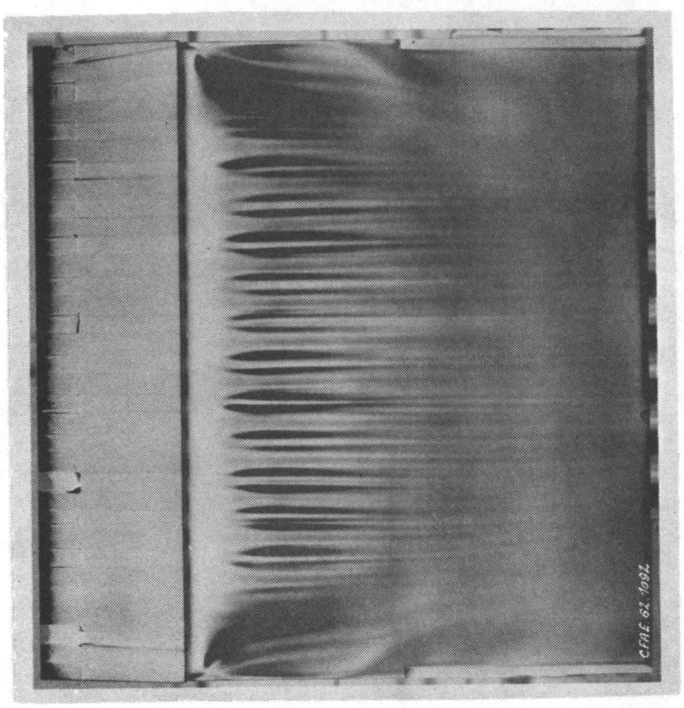

b) WITH TAPES.

FIGURE 18. SUBLIMATION PICTURE WITH AND WITHOUT PIECES OF SCOTCH TAPES AT THE LEADING EDGE OF THE MODEL - M = 2.25.

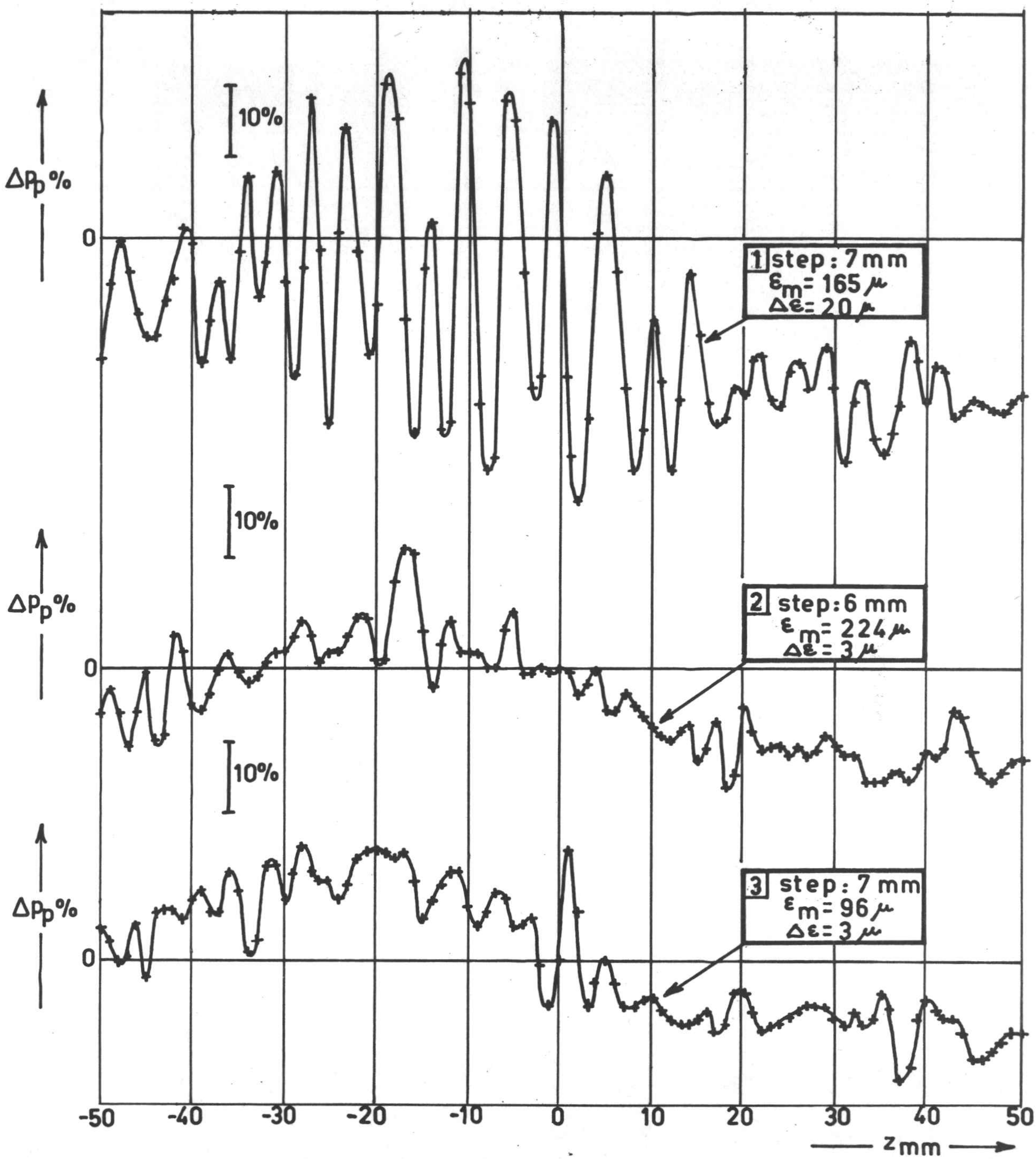

FIGURE 19 - Spanwise variations of pitot pressure demonstrating the leading edge effect

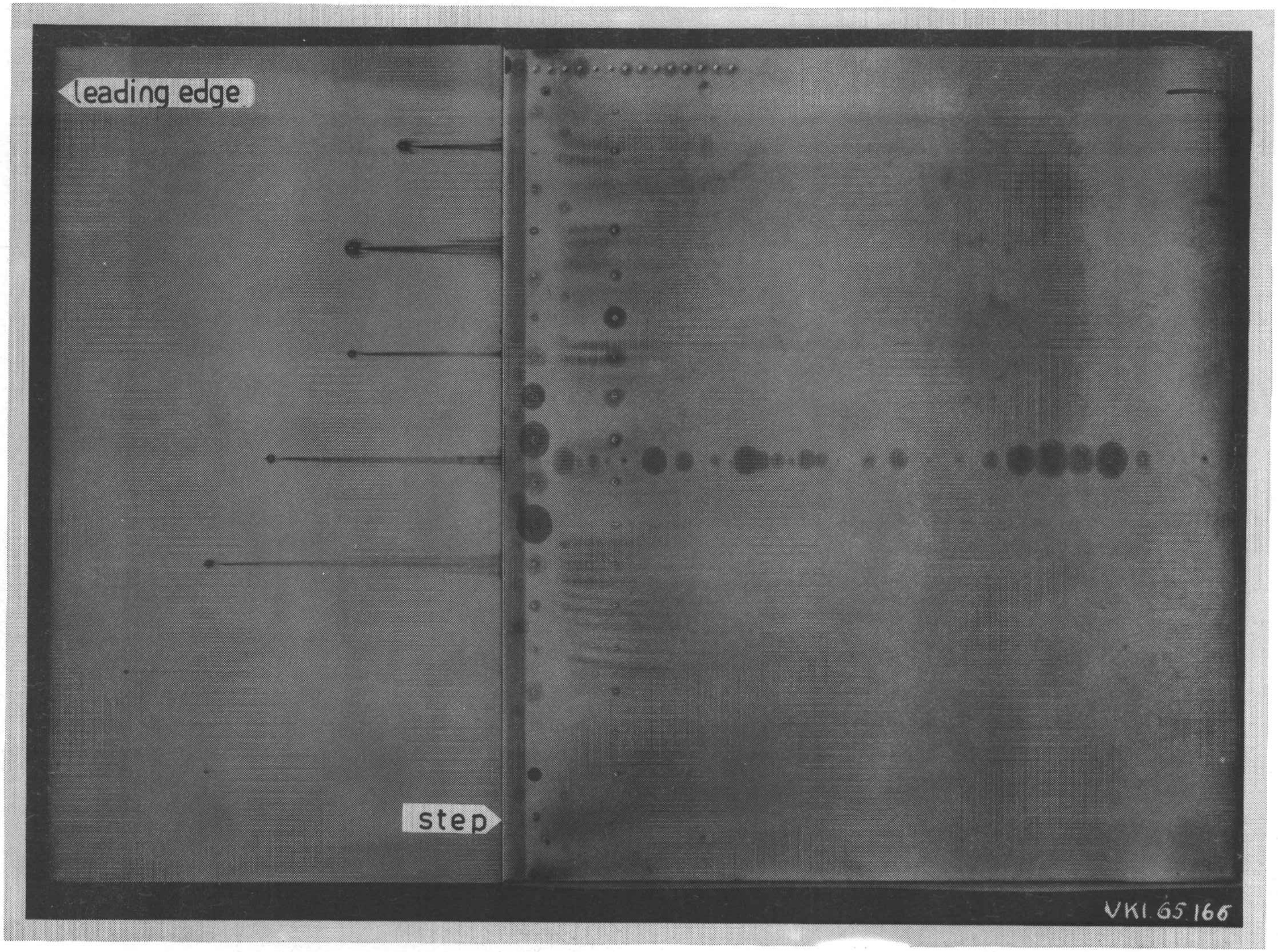

FIGURE 20. SUBLIMATION PICTURE SHOWING THE EFFECT OF ROUGHNESS ELEMENTS.

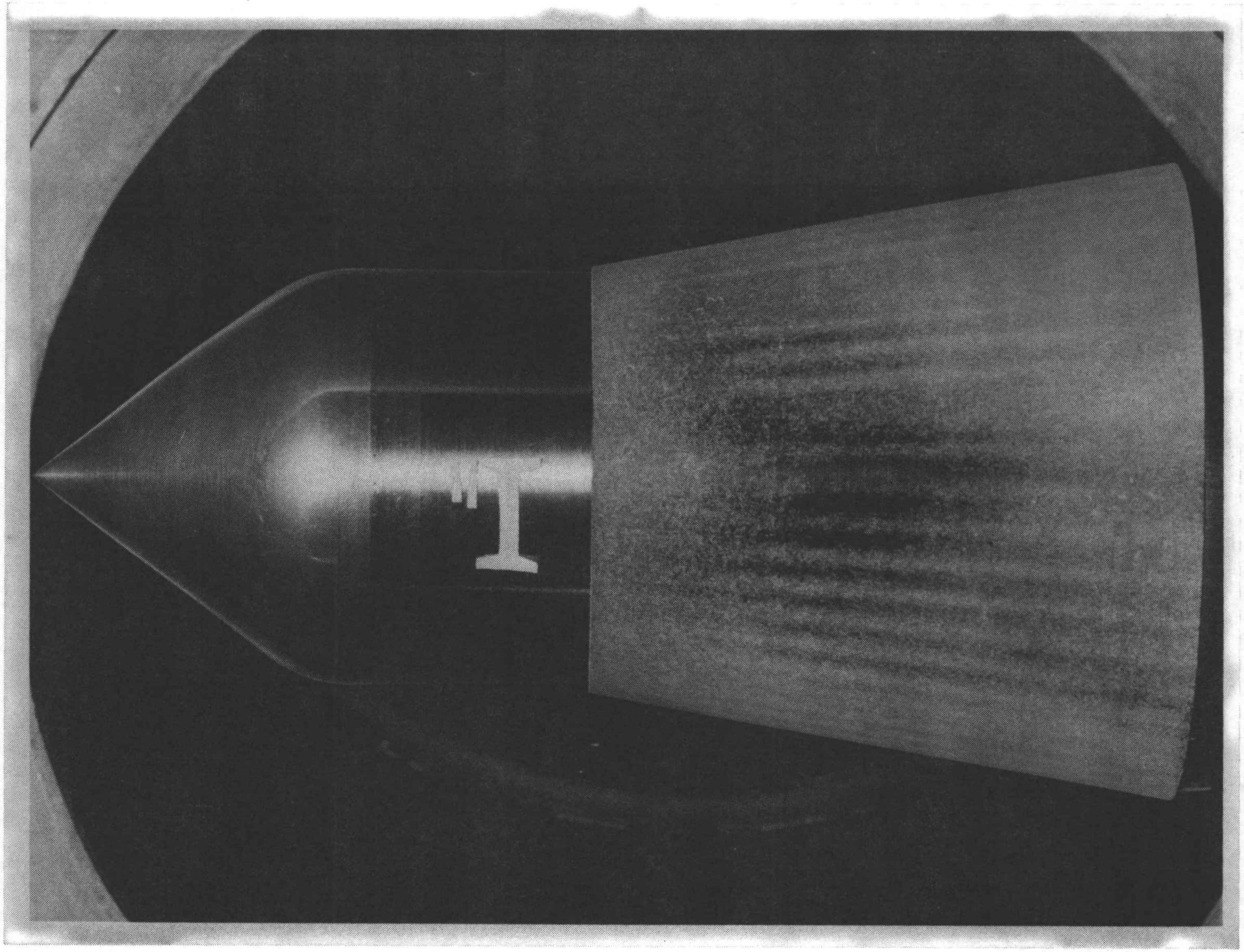

FIGURE 21. SUBLIMATION PICTURE OF A FLARED AXI-SYMMETRIC BODY WITH "ARTIFICIAL" STREAMWISE VORTICES AT M= 2,25.

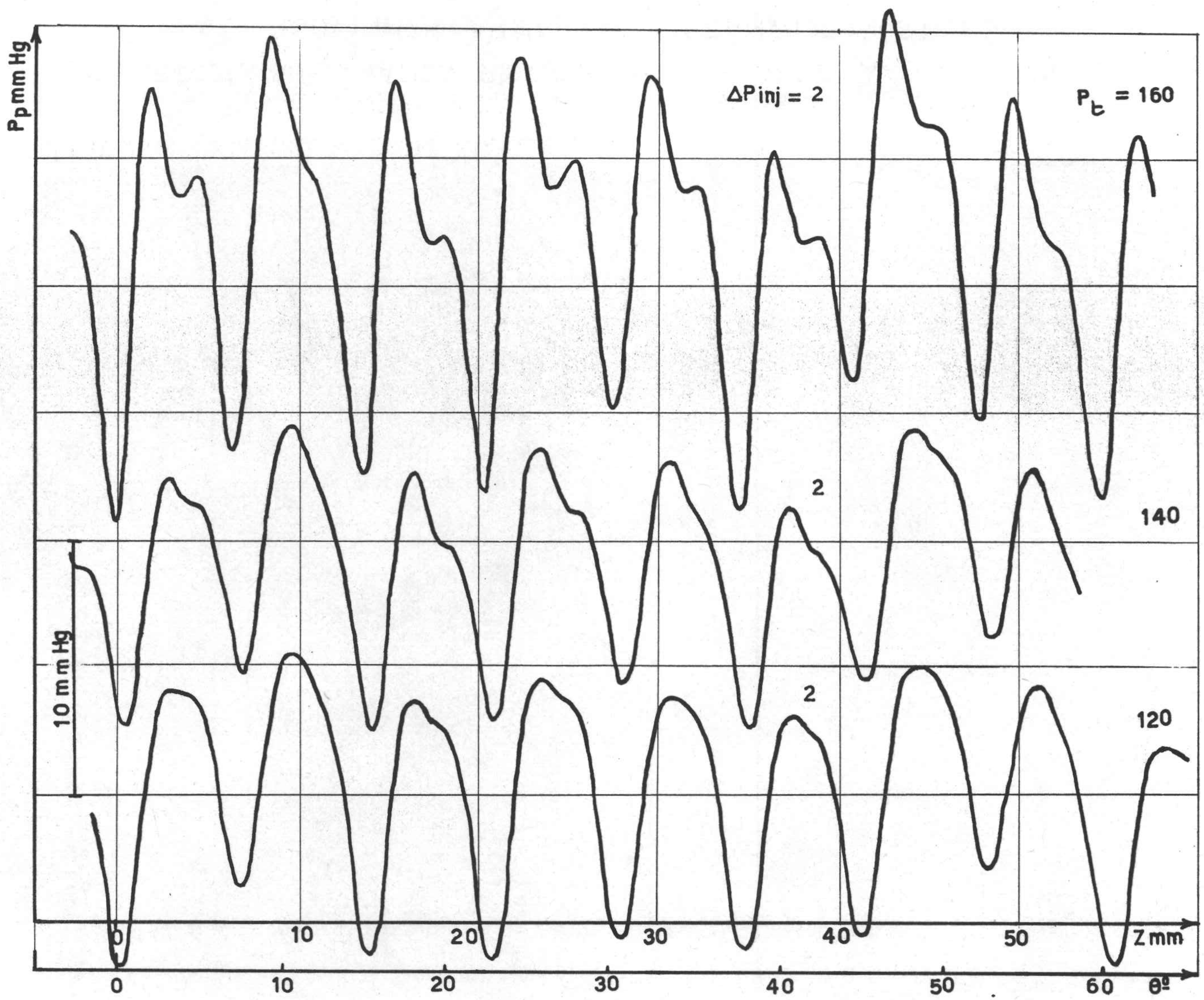

FIGURE 22_Spanwise variations of pitot pressure on flare of the model shown in figure 21

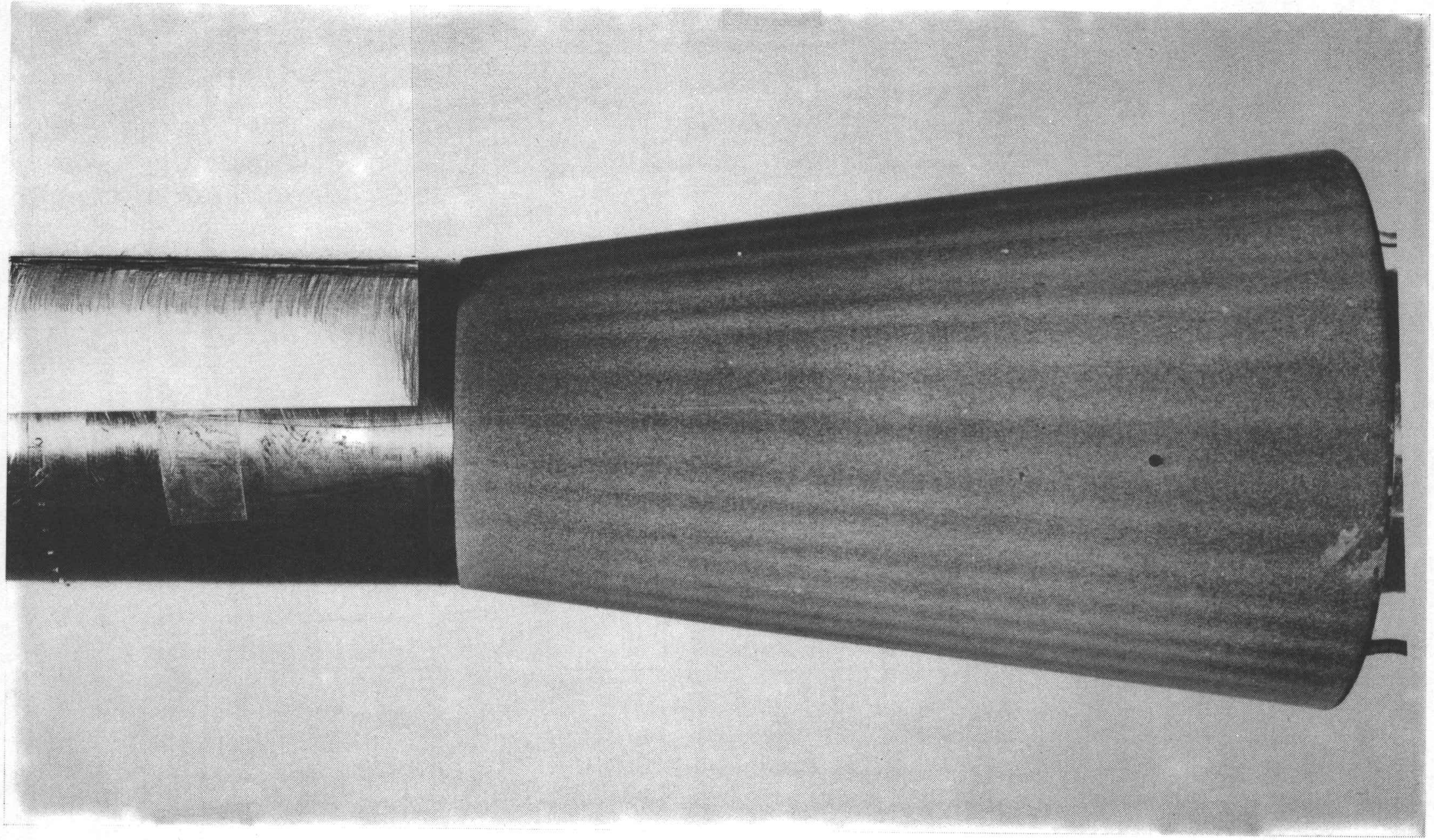

FIGURE 23. SUBLIMATION PICTURE OF A FLARED AXI-SYMMETRIC BODY WITH "ARTIFICIAL" STREAMWISE VORTICES AT M=5.3 .

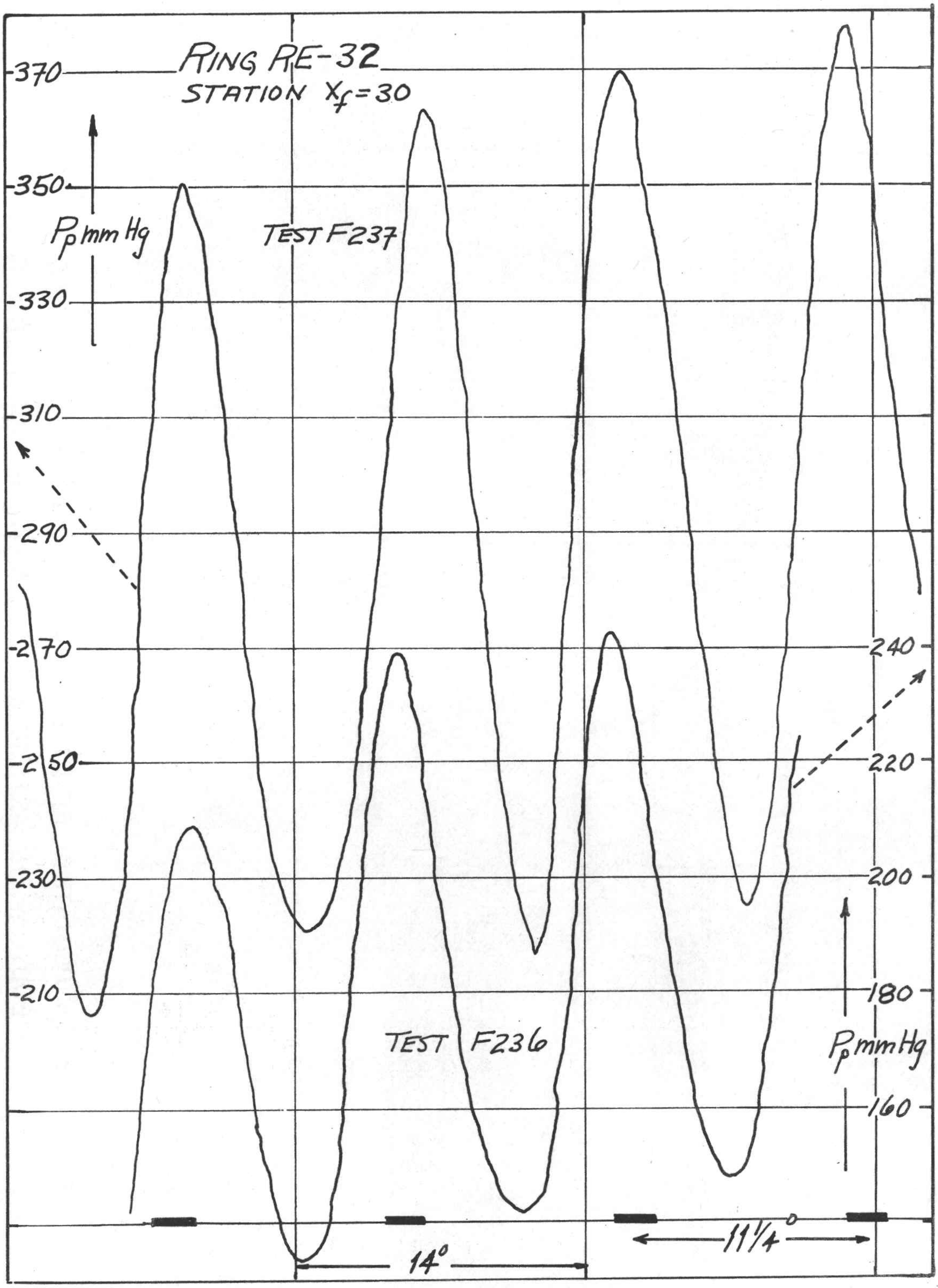

FIGURE 24_Spanwise variations of pitot pressure on the flare of the model shown in figure 23

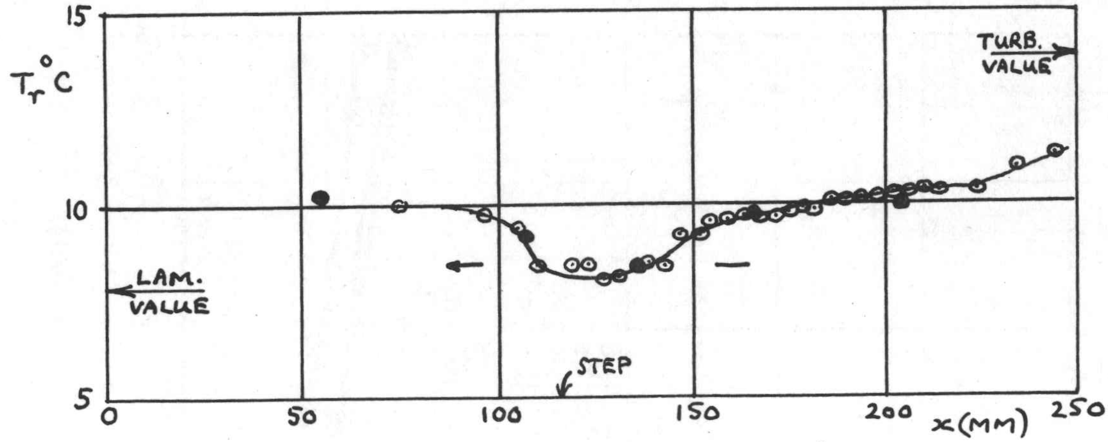

a. 2·7 MM. STEP MODEL (BFS-2). ALL Re.

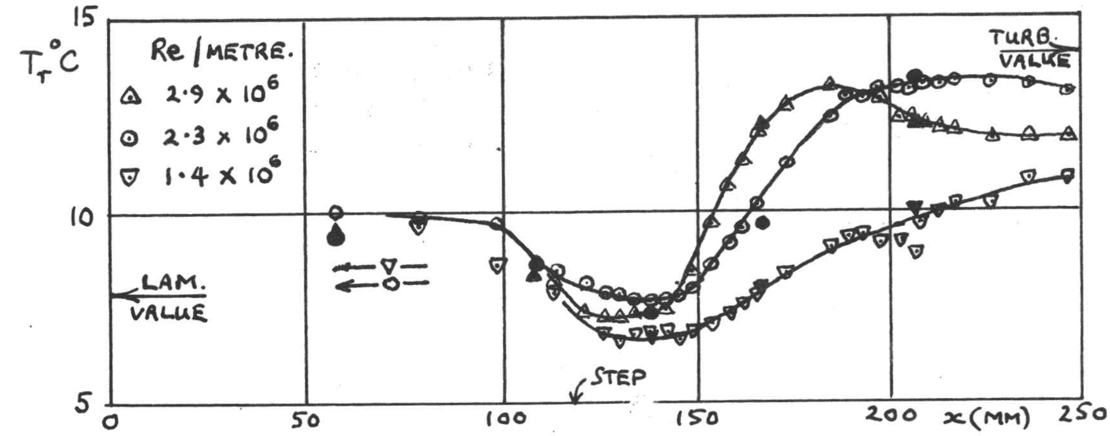

b. 5·1 MM. STEP MODEL (BFS-1).

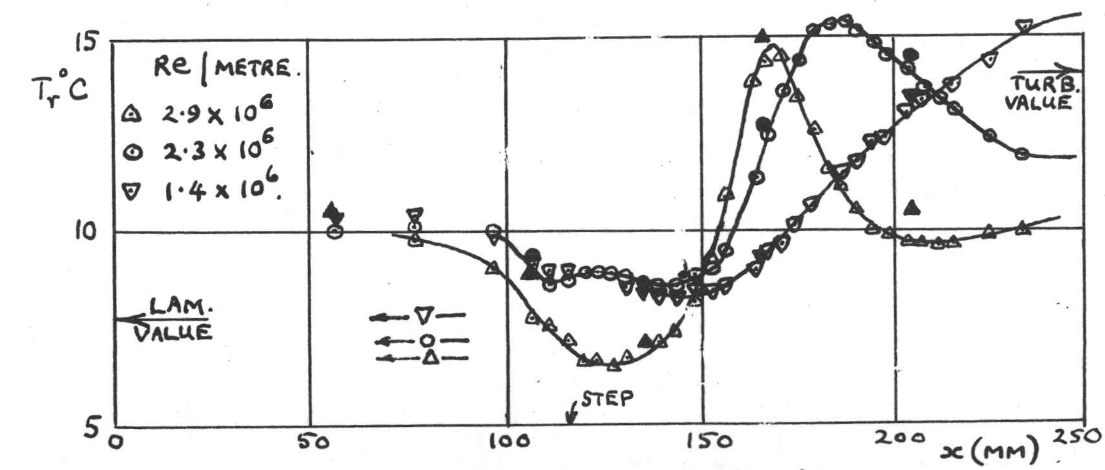

c. 6·8 MM. STEP MODEL (BFS-3).

FIGURE 25_Recovery temperature distributions over backward facing step models at M = 2.02

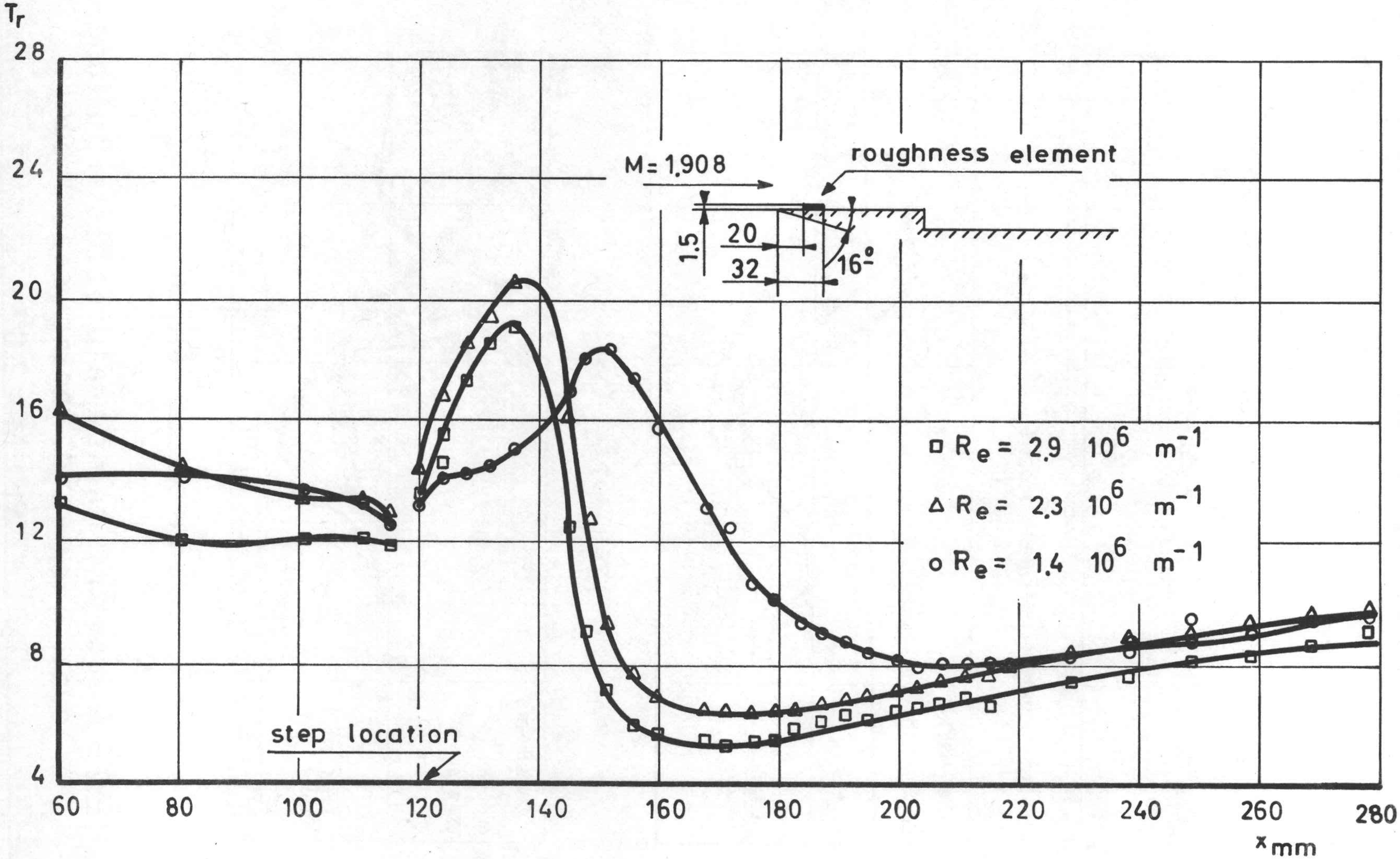

Fig. 26 _ RECOVERY TEMPERATURE DISTRIBUTION WITH A TURBULENT BOUNDARY LAYER AT SEPARATION, 6,8 mm step, T_o = 300° K.

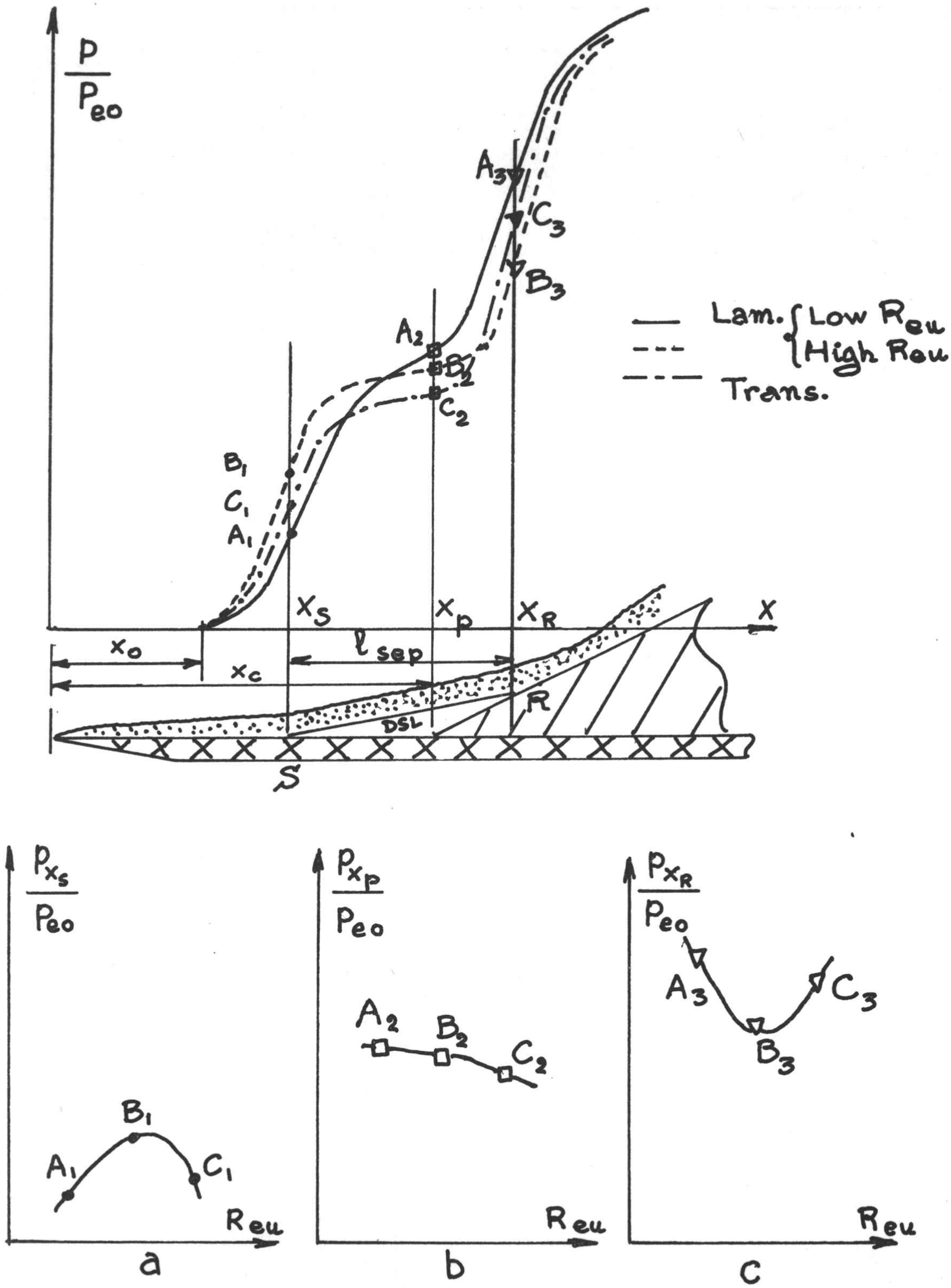

FIGURE 27_Criterion for detecting transition PRINCIPLE

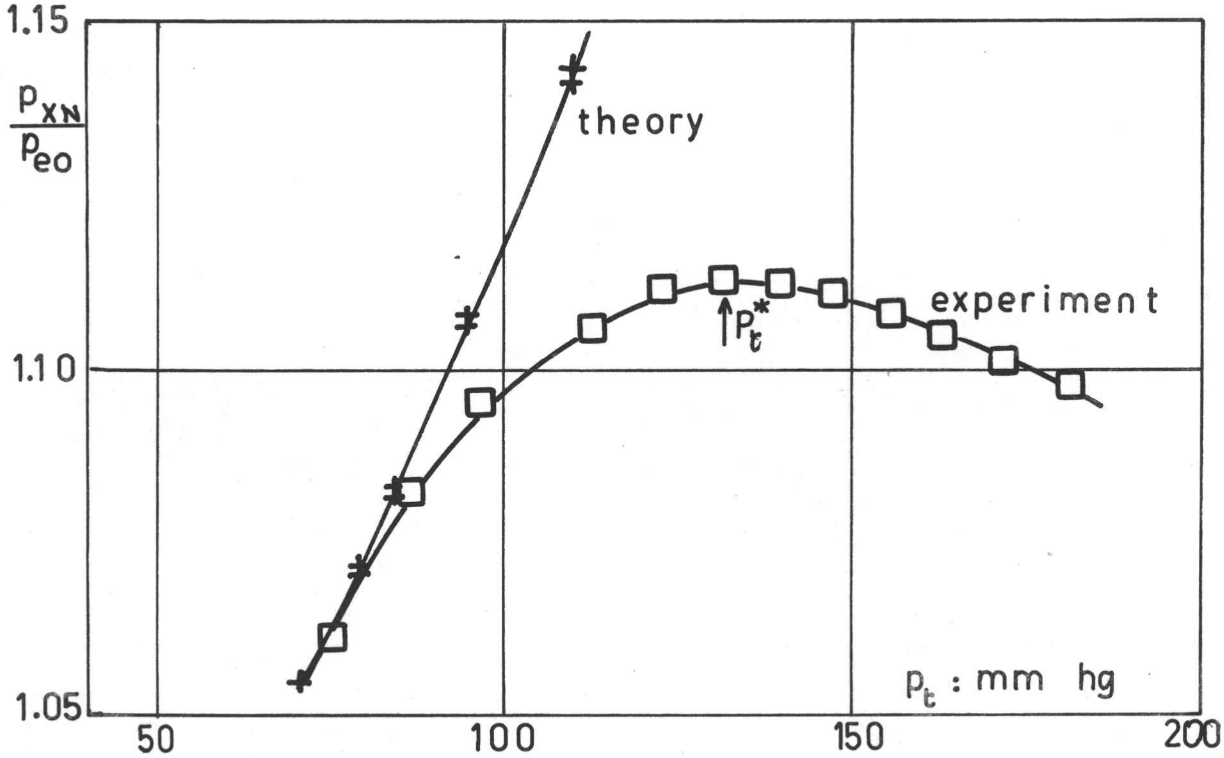

FIGURE 28 _ Criterion for detecting transition (10° flap) M=2.25

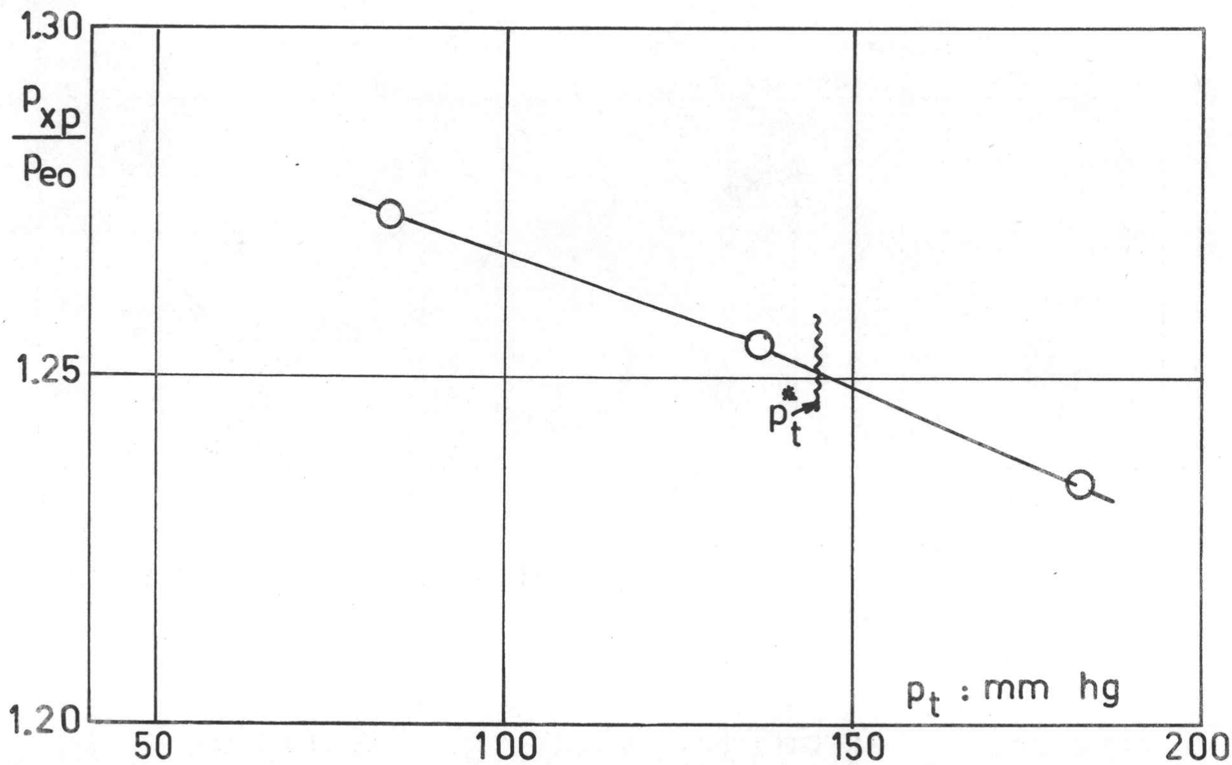

FIGURE 29 _ Separated flow pressure variation with p_t (10° flap)

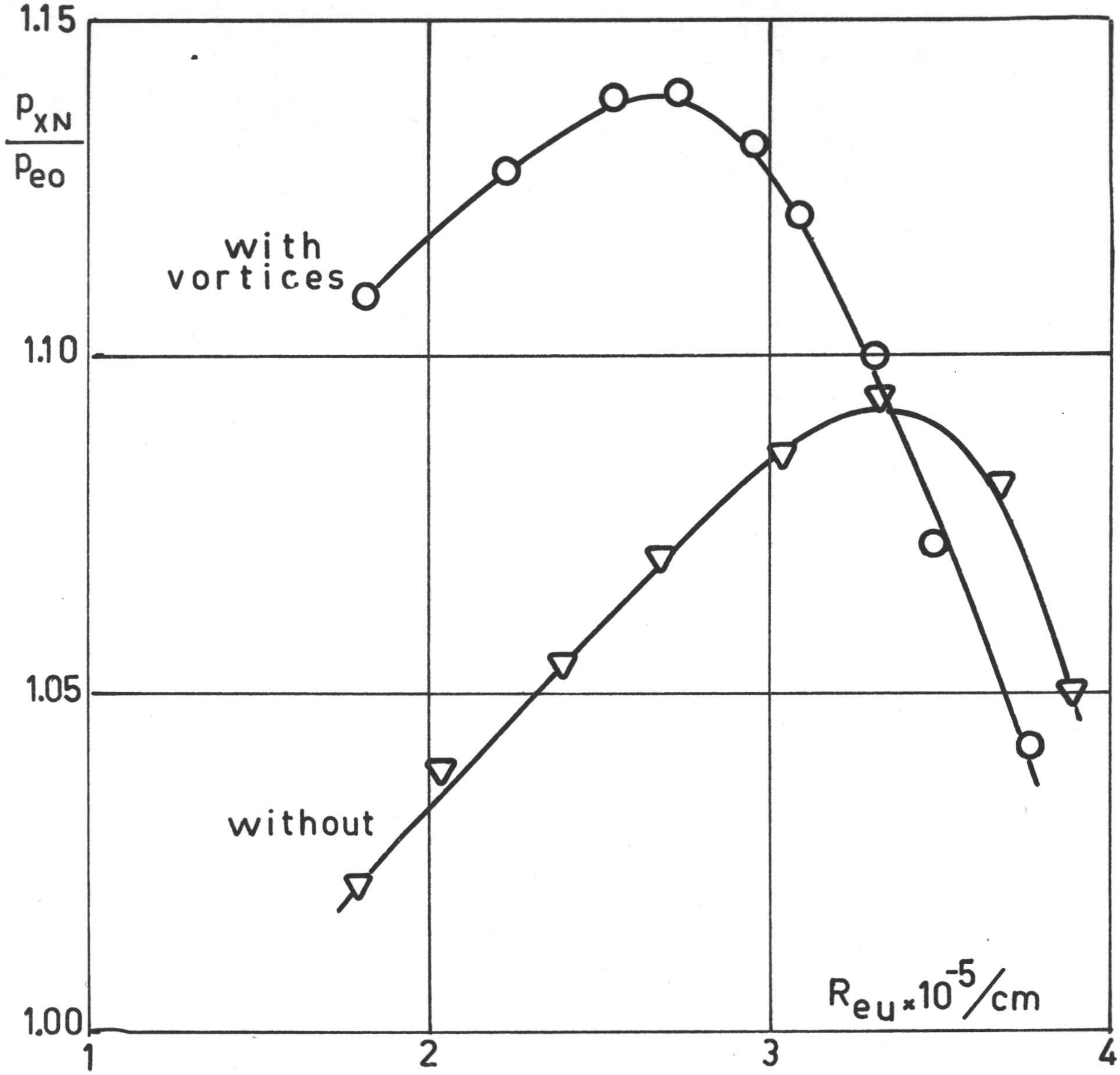

FIGURE 30_Effect of streamwise vorticies on transition

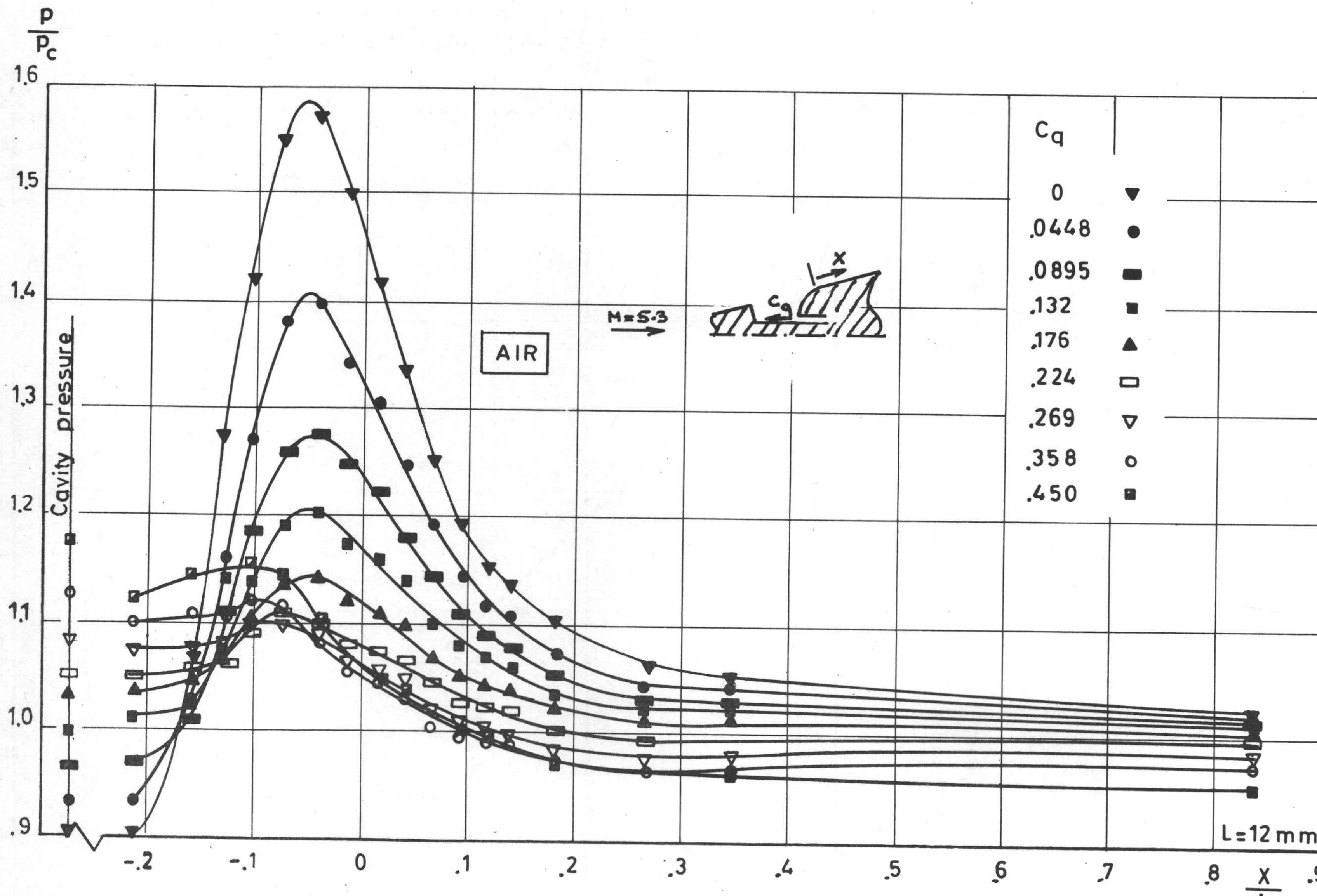

FIGURE 31_ Static pressure distributions near reattachment on cone-cavity

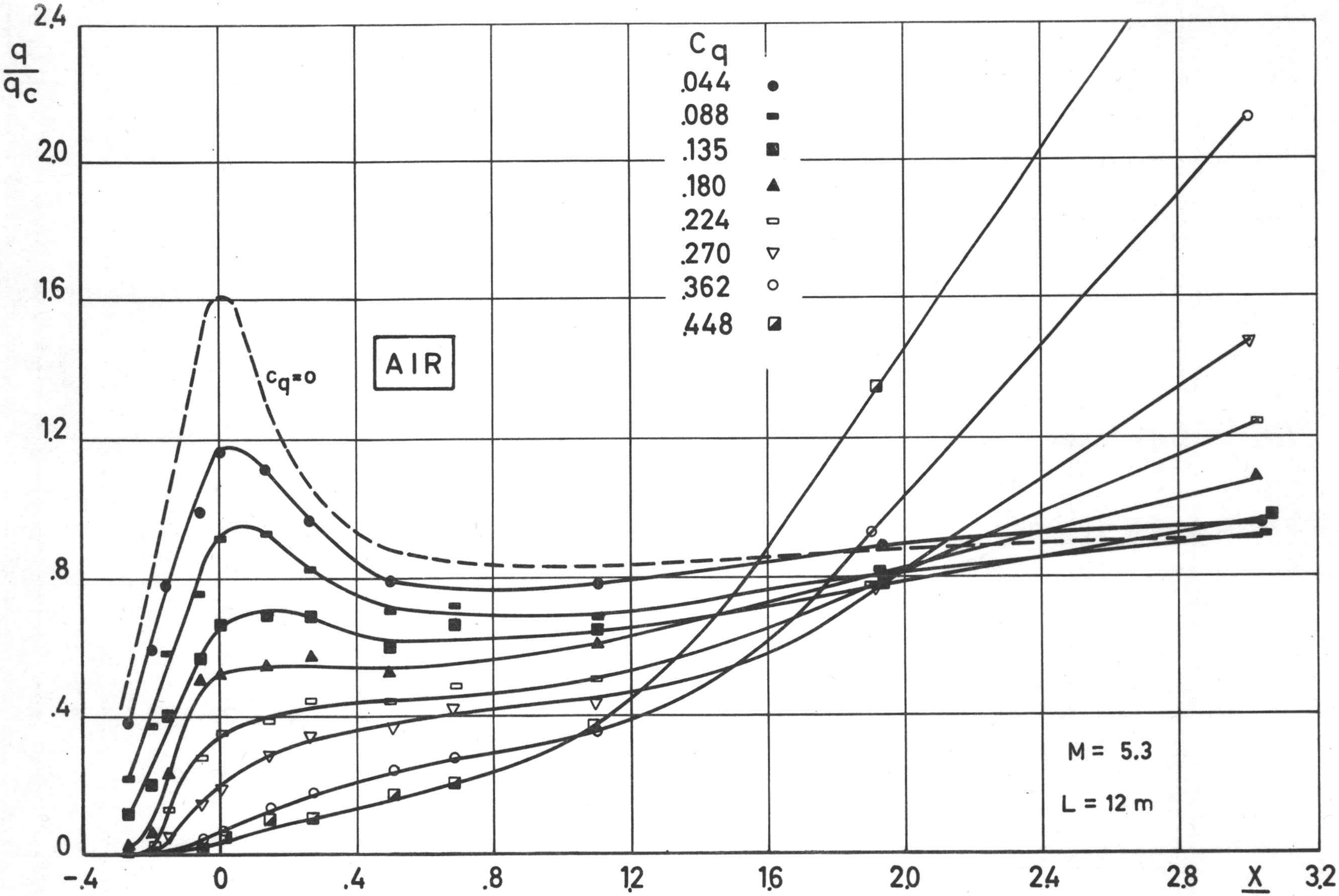

FIGURE 32_Heat transfer distributions near reattachment on a cone cavity model

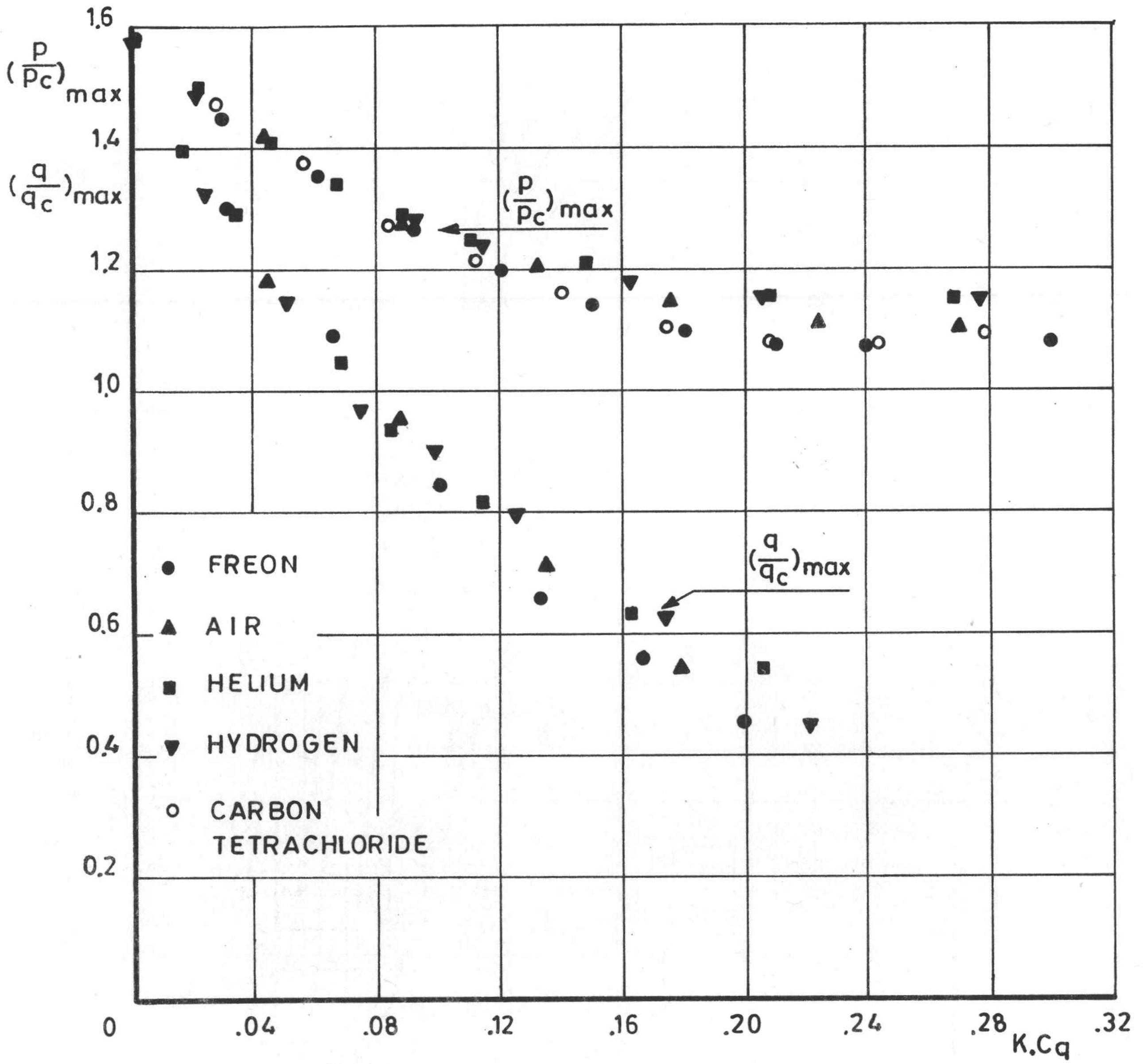

Fig. 33 CORRELATED PRESSURE AND HEAT TRANSFER PEAK RATIOS.

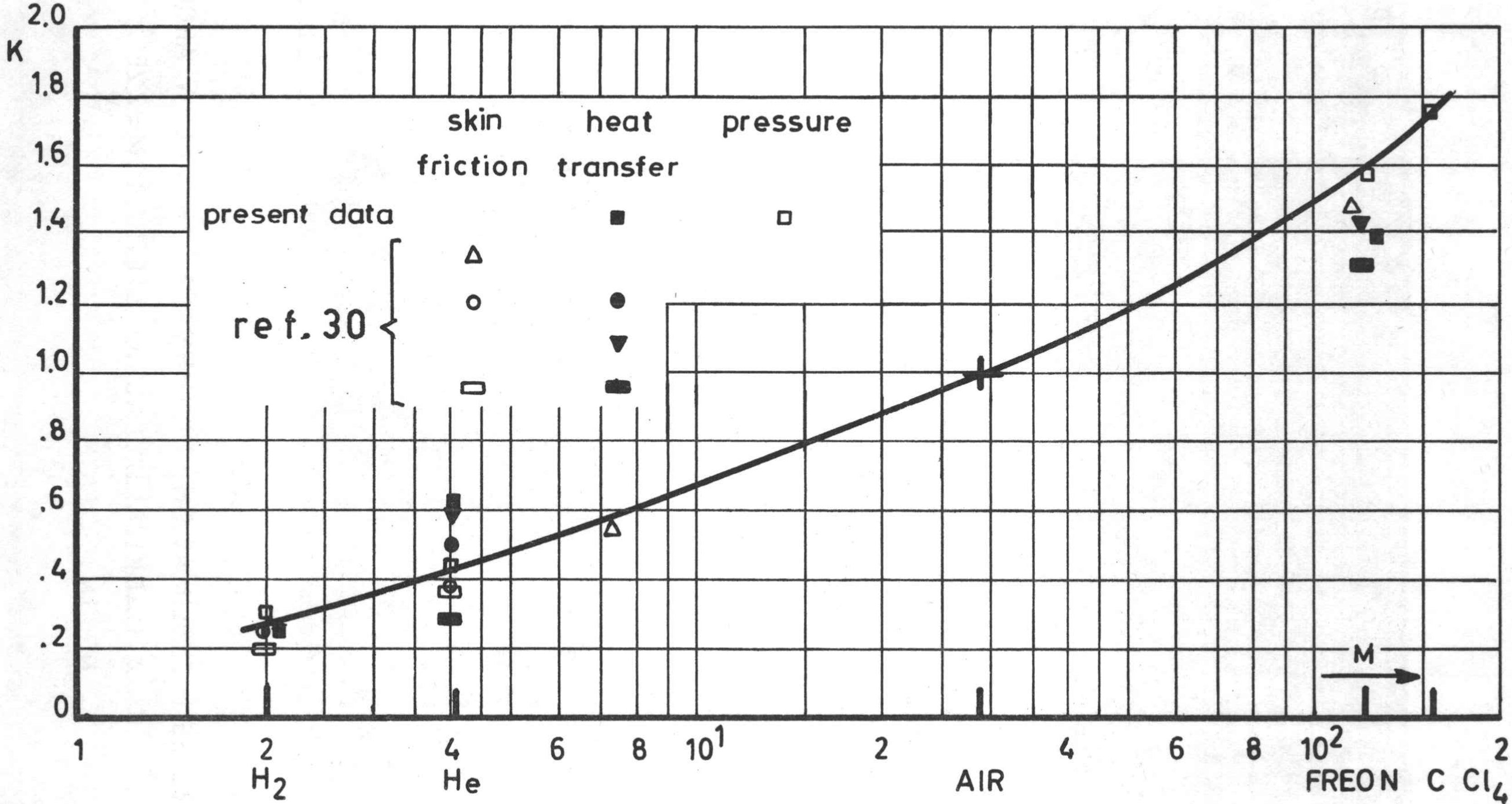

Fig. 34 - CORRELATION FACTOR K VERSUS MOLECULAR WEIGHT.

FIGURE 35. SUBLIMATION PICTURE OF THE FLOW AROUND A BACKWARD FACING STEP AT M = 2.25 NO INJECTION.

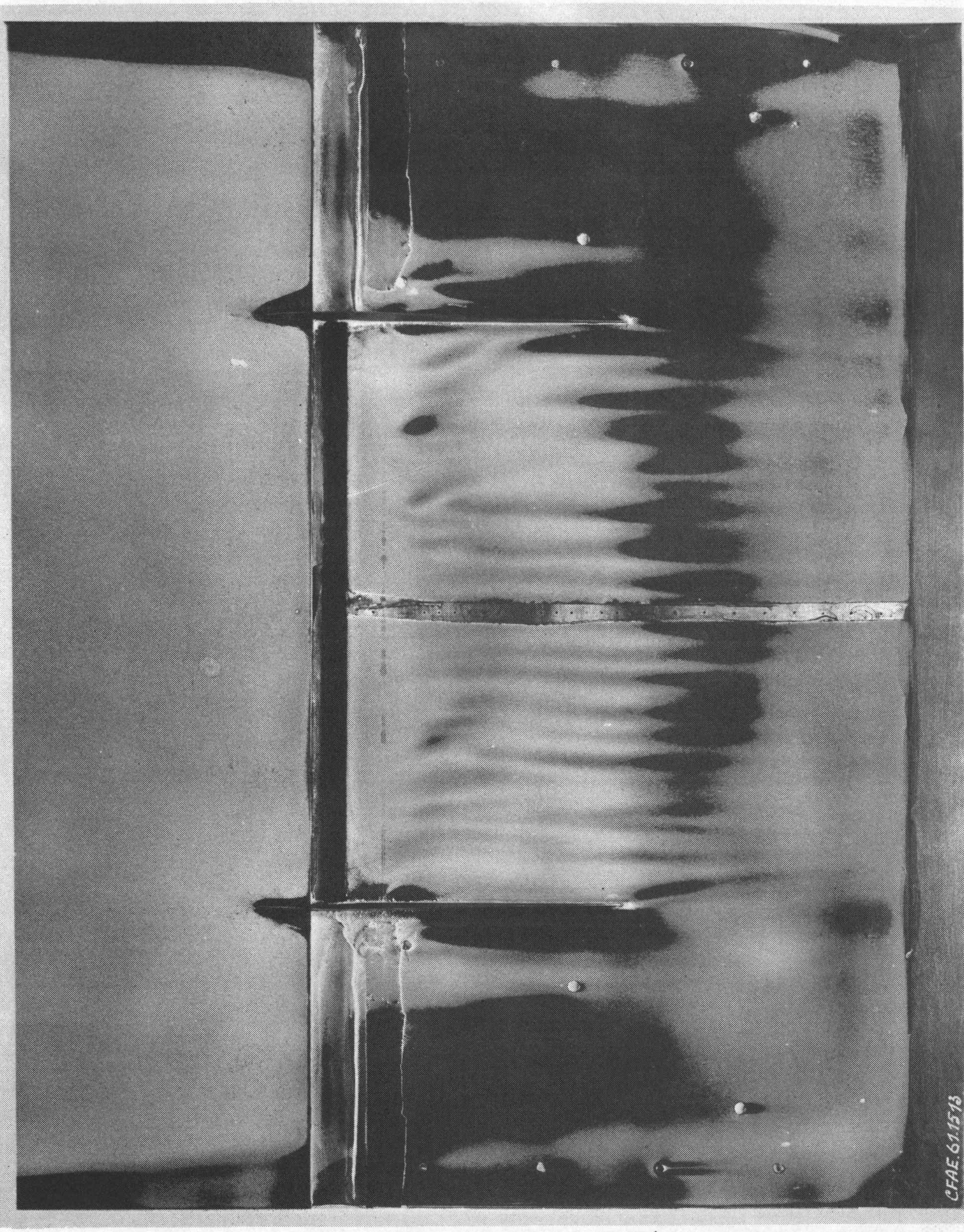

FIGURE 36. SUBLIMATION PICTURE OF THE FLOW AROUND A BACKWARD FACING STEP AT M=2.25. MODERATE INJECTION.

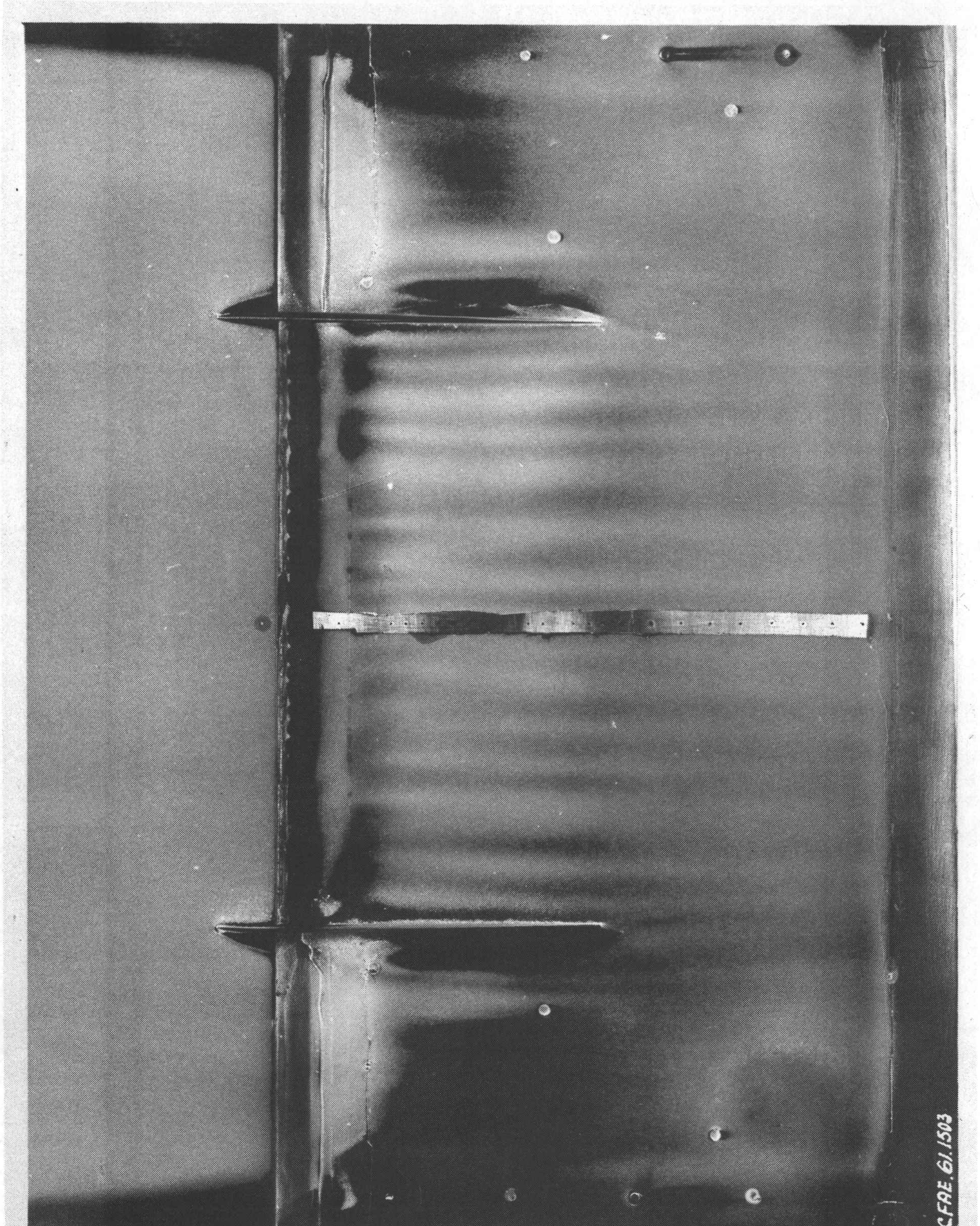

FIGURE 37. SUBLIMATION PICTURE OF THE FLOW AROUND A BACKWARD FACING STEP AT M = 2.25. LARGE INJECTION.